Design and Synthesis of Imidazole Functionalized Donor–Acceptor Systems

M.Sc. Thesis

By

Harshal Thaker



DEPARTMENT OF CHEMISTRY

INDIAN INSTITUTE OF TECHNOLOGY INDORE

MAY 2026

Design and Synthesis of Imidazole Functionalized Donor–Acceptor Systems

A THESIS

Submitted in partial fulfillment of the
requirements for the award of the degree
of
Master of Science

by

Harshal Thaker



DEPARTMENT OF CHEMISTRY
INDIAN INSTITUTE OF TECHNOLOGY INDORE
MAY 2026

INDIAN INSTITUTE OF TECHNOLOGY INDORE

CANDIDATE'S DECLARATION

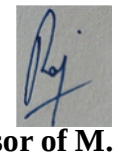
I hereby declare that the work which is being presented in the thesis **Design and Synthesis of Imidazole Functionalized Donor–Acceptor Systems** in the partial fulfillment of the requirements for the award of the degree of **MASTER OF SCIENCE** and submitted in the **DEPARTMENT OF CHEMISTRY, Indian Institute of Technology Indore**, is an authentic record of my own work carried out during the time period from July 2025 to May 2026 of M.Sc. Thesis submission under the supervision of **Prof. Rajneesh Misra**, Senior Professor, IIT Indore. The matter presented in this thesis has not been submitted by me for the award of any other degree at this or any other institute.

21/05/2026

Signature of the student with date

(Harshal Thaker)

This is to certify that the above statement made by the candidate is correct to the best of my/our knowledge.



Signature of the Supervisor of M.Sc. thesis

(Prof. Rajneesh Misra)

Harshal Thaker has successfully given the oral his M.Sc. The oral examination was held on **21 May 2026**.



Signature(s) of Supervisor(s) of MSc thesis
Date: 21/05/2026

ACKNOWLEDGEMENTS

With great pleasure, I want to express my deep sense of gratitude to my supervisor Prof. Rajneesh Misra, for giving me a wonderful opportunity to pursue research and for believing in my research abilities. His constant guidance, support and motivation have been immensely helpful to complete this M.Sc. project. His enthusiasm and dedication have always inspired me. Further, I would like to thank my PSPC members Prof. Sampak Samanta and Dr. Chelvam Venkatesh for their valuable suggestions and support.

I wish to express my gratitude to Prof. Suhas S. Joshi, Director, IIT Indore for his continuous encouragement, help, and support in every aspect. I am grateful to Dr Umesh A. Kshirsagar (Head, Department of Chemistry, Indian Institute of Technology Indore). I am also grateful to Prof. Suman Mukhopadhyay, Prof. Sanjay Singh, Prof. Apurba Kumar Das, Dr. Amrendra Kumar Singh, Prof. Shaikh M. Mobin, Prof. Anjan Chakraborty, Prof. Satya S. Bulusu, Prof. Tushar Kanti Mukherjee, Dr. Tridib Kumar Sarma, Dr. Selvakumar Sermadurai, Dr. Abhinav Raghuvanshi, Dr. Deepak Kumar Roy and Dr. Umesh Kshirsagar, for the help during various activities.

I would like to extend my sincere thanks to my mentor, Vivak Kandpal, for his supportive, kind and friendly nature. I extend my deep thanks to my group members, Dr Mohd. Wazid, Dr Nikhil Ji Tiwari, Ramakant Gavale, Amiy Krishna, Nitin Rajesh, Kusum, Shivangi Tiwari, Akanksha Dwivedi, Kushagra P. Rana, Anurag Kumar Mishra, Dhruv Jasoliya and Prashant Kumar for their selfless co-operation and help to make my work successful. I would also like to thank the technical staff from the Sophisticated Instrumentation Centre (SIC), IIT Indore, Mr. Kinny Pandey and Mr. Ghanshyam Bhavsar for their patience and timely technical support without which it was impossible to continue with my work. I personally want to extend my thanks to my batch mates who were always there and never let me down during these M.Sc. days.

Here, it is to be specially mentioned that, none of this would have been possible without the support of my family and I deeply express my love and gratitude to my parents. Finally, I would like to express my thanks to IIT Indore for its infrastructure and all others who have helped and supported me directly and indirectly.

Harshal Thaker

DEDICATION

Every challenging work needs self-endeavour and the blessings of elders.

My modest effort I dedicate to my concern and supporting

FAMILY

Whose motivation, love, and encouragement

make me able to complete my work efficiently.

Along with all inspiring and respected

TEACHERS

ABSTRACT

Dianisole (DAn) and fluorene (Flu) functionalised 4,5-diphenylimidazole based donor-acceptor systems, **Imd-DAn** and **Imd-Flu** were synthesised *via* Suzuki and Buchwald-Hartwig cross-coupling reactions in good yields. **Imd-DAn** exhibits red-shifted absorption and emission compared to **Imd-Flu**, which is attributed to the stronger electron-donating ability and enhanced conjugation of the DAn unit. **Imd-DAn** and **Imd-Flu** were characterised using ^{1}H NMR, ^{13}C NMR and HRMS techniques. Furthermore, DFT calculations demonstrated that the HOMO is mainly localised on the imidazole core and donor units, whereas the LUMO is delocalized over the entire molecular framework. The results demonstrated the potential of such donor-acceptor systems for future optoelectronic applications, particularly in organic light-emitting devices (OLEDs) and in sensing.

TABLE OF CONTENTS

	LIST OF FIGURES	vi-vii
	LIST OF SCHEMES	viii
	ABBREVATIONS	ix
	ACRONYMS	x
Chapter 1	**INTRODUCTION**	1-4
Chapter 2	**LITERATURE REVIEW**	5-6
Chapter 3	**EXPERIMENTAL SECTION**	7-9
Chapter 4	**RESULTS AND DISCUSSION**	10-15
Chapter 5	**CONCLUSION**	16
	APPENDIX-A	17-25
	REFERENCES	26

LIST OF FIGURES

Figure 1.	Structural variations in the bonding connectivity of the imidazole ring	2
Figure 2	The molecular structure **Imd-Flu** and **Imd-DAn**	4
Figure 3	Structures of triphenylimidazole-based OLED emitters **Imd–1-NaCBI** and **Imd-2-NaCBI** with enhanced electroluminescent performance.	5
Figure 4	Structures of ESIPT-based imidazole dyes **Imd-HPI** and **Imd-m-MHPI** for full-colour emission applications.	6
Figure 5	UV-visible spectra of **Imd-Flu** and **Imd-DAn** in DCM.	13
Figure 6	Fluorescein spectra of **Imd-Flu** and **Imd-DAn** in DCM.	13
Figure 7	The frontier molecular orbitals of the **Imd-Flu** and **Imd-DAn**.	14
Figure 8	Energy level diagram of **Imd-Flu** and **Imd-DAn.**	15
Figure 9	^{1}H NMR of Compound **DAn (3)**.	17
Figure 10	^{13}C NMR of Compound **DAn (3)**.	18
Figure 11	HRMS of Compound **DAn (3)**.	18
Figure 12	^{1}H NMR of Compound **Imd-Br$_2$ (7)**.	19
Figure 13	^{13}C NMR of Compound **Imd-Br$_2$ (7)**.	20
Figure 14	HRMS of Compound **Imd-Br$_2$ (7)**.	20
Figure 15	^{1}H NMR of Compound **Flu-Bpin (9)**.	21
Figure 16	^{13}C NMR of Compound **Flu-Bpin (9)**.	21
Figure 17	HRMS of Compound **Flu-Bpin (9)**.	22
Figure 18	^{1}H NMR of Compound **Imd-DAn**.	22
Figure 19	^{13}C NMR of Compound **Imd-DAn**.	23
Figure 20	HRMS of Compound **Imd-DAn**.	23
Figure 21	^{1}H NMR of Compound **Imd-Flu**.	24

Figure 22	^{13}C NMR of Compound **Imd-Flu**.	24
Figure 23	HRMS of Compound **Imd-Flu**.	25

LIST OF SCHEMES

Scheme 1	Synthesis route of Compound **3**.	10
Scheme 2	Synthesis route of Compound **7**.	10
Scheme 3	Synthesis route of Compound **9**.	11
Scheme 4	Synthesis route of Compound **Imd-Flu**.	11
Scheme 5	Synthesis route of Compound **Imd-DAn.**	12

ABBREVIATIONS

mg	Milligram
mol	Mole
g	Gram
℃	Degree Celsius
%	Percentage
h	Hours
min	Minutes
mL	Milliliter
π	Pi
λ	Wavelength
δ	Chemical shift
eV	Electron volt
V	Volt

ACRONYMS

Abbreviations used here for substituents, reagents, etc. are largely in accordance with the recommendation of the IUPAC-IUC Commission on Biochemical Nomenclature, 1974, Pure and Applied Chemistry, 40, 315-331. Additional abbreviations used in this report are listed below:

OLEDs	Organic Light Emitting Diodes
HOMO	Highest Occupied Molecular Orbitals
LUMO	Lowest Unoccupied Molecular orbitals
RGB	Red-Green-Blue
1-NaCBI	1-Napthyl-benzaimidazole
2-NaCBI	2-Napthyl-benzaimidazole
BUBD-1	Blue fluorescent dopant material
DFT	Density functional theory
HRMS	High-resolution mass spectrometry
CIE	Commission Internationale
HPI	Hydroxyphenyl Imidazole
m-MHPI	meta methoxy hydroxyphenyl imidazole
NMR	Nuclear magnetic resonance
TMS	Tetramethylsilane
DAn	Di-anisole
Flu	Fluorene

Chapter 1 Introduction

1.1. General Introduction

Recently, organic π-conjugated materials have attracted significant scientific interest owing to their versatile applicability in advanced electronic and optoelectronic devices such as organic thin-film transistors (OTFTs), organic light-emitting diodes (OLEDs), photovoltaic devices, and chemical and biological sensors.[1–3] Among the various molecular design strategies, donor-acceptor (D–A) architectures have emerged as one of the most effective approaches for tuning optoelectronic properties.[4]

In the donor–acceptor systems, electron-rich donor units are covalently connected to electron-deficient acceptor moieties, enabling efficient intramolecular charge transfer (ICT) interactions.[5] Such interactions effectively tune the absorption and emission characteristics, electronic band gap, charge-transport properties and excited-state dynamics of the molecules. Consequently, D–A systems have been extensively explored for high-performance optoelectronic and photonic applications.[6] In particular, the donor-π-acceptor (D–π–A) systems containing conjugated π-linkers have gained immense attention because the π-spacer facilitates effective electronic communication between donor and acceptor units, enhances electron delocalisation, reduces steric hindrance and enables precise modulation of molecular energy levels.[8] The incorporation of π-conjugated bridges also improves light-harvesting ability, fluorescence behaviour and charge-transfer efficiency, thereby enhancing the overall photophysical and electrochemical performance of the materials. D–π–A molecular systems have been widely investigated for OLEDs, organic photovoltaics, nonlinear optical materials, fluorescent probes, and sensing applications.[9–10]

Imidazole has emerged as a highly promising heterocyclic framework for the development of donor–acceptor systems because of its unique electronic structure, excellent thermal stability, facile synthetic accessibility and tunable photophysical properties.[11] Imidazole is a five-membered aromatic heterocycle containing two nitrogen atoms with distinct electronic characteristics. The N1 atom behaves as a pyrrole-like nitrogen and its lone pair participates in the aromatic π-sextet, while, N3 atom behaves as a pyridine-like nitrogen with its lone pair localized in an sp^2 orbital and not involved in aromaticity.[12] This dual electronic nature imparts bipolar characteristics to the imidazole framework, enabling it to exhibit both

electron-donating and electron-accepting behaviour depending on the substitution pattern. An important advantage of the imidazole framework is its remarkable synthetic versatility. Imidazole core can be easily functionalized at the N1, C2, C4 and C5 positions, allowing tuning of electronic and steric properties (Figure 1). Imidazole derivatives generally exhibit high thermal and chemical stability, strong fluorescence, efficient charge-transport capability and tunable emission behaviour.[13] In comparison to traditional organic luminophores that suffer from aggregation-caused quenching (ACQ) in the solid state, the imidazole-based fluorophores retain strong emission in both solution and aggregated states. This makes imidazole derivatives attractive candidates for optoelectronic and photonic applications including OLEDs, organic photovoltaics, fluorescent chemosensors, pH sensors, electron-transfer systems, bioimaging, anti-counterfeiting materials and latent fingerprint detection.[14]

A variety of imidazole-based luminophores such as benzilimidazole, 4,5-diphenylimidazole, triphenylimidazole, tetraphenylimidazole, phenanthroimidazole, imidazo[1,5-a]pyridine, and pyrenoimidazole derivatives, have been extensively investigated because of their excellent optical and electronic properties.[15] Recent studies have demonstrated that molecular engineering through donor substitution, π-conjugation extension and structural rigidification can significantly improve the fluorescence efficiency, colour tunability, charge mobility, and solid-state emission behaviour of imidazole-based systems.[16] Furthermore, the introduction of donor groups into imidazole-based architectures can facilitate strong ICT interactions and induce solvatochromic behaviour, making them useful for sensing and imaging applications.[17]

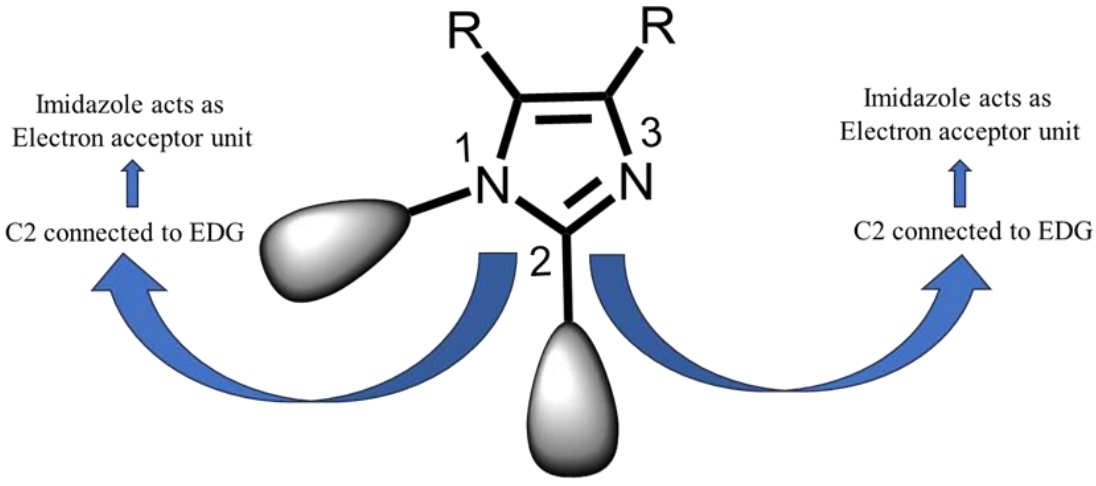


Figure 1. Structural variations in the bonding connectivity of the imidazole ring.

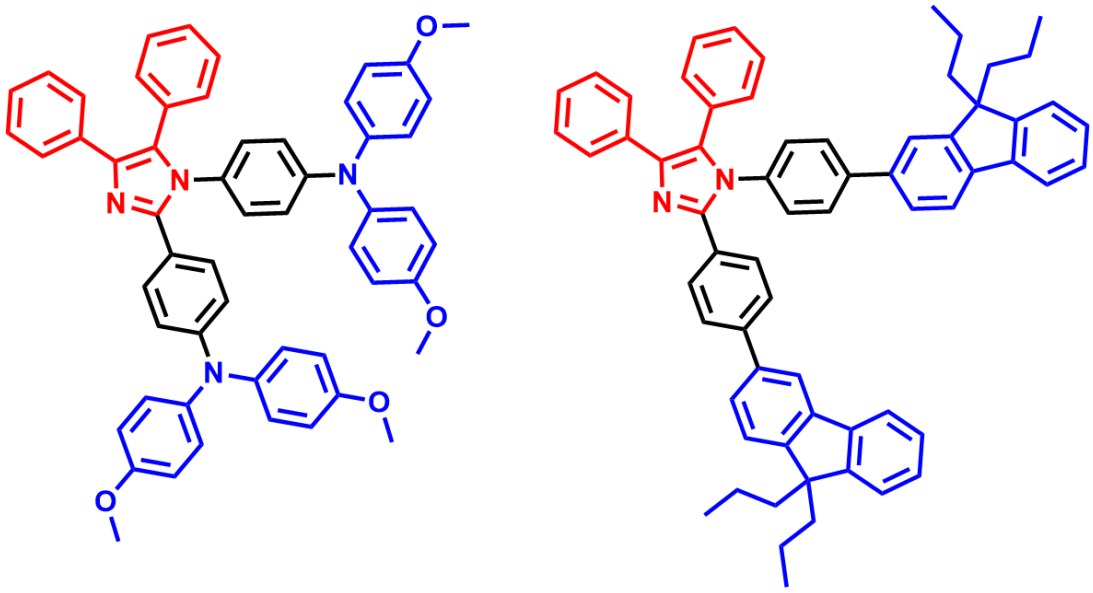
Fluorene (Flu) is π-conjugated building block widely used in optoelectronics. Structurally, fluorene is a rigid polycyclic aromatic hydrocarbon composed of two benzene rings fused to a central five-membered ring containing a methylene bridge at the 9-position.[18] This rigid and planar architecture provides excellent thermal stability, high fluorescence quantum yield and efficient charge-transport characteristics. Fluorene can be readily functionalized at the 2,7-positions as well as at the 9-position, enabling structural modifications for tuning the optoelectronic properties.[19] Due to excellent hole-transporting ability and blue-emissive nature, fluorene derivatives have been widely used in OLEDs, conjugated polymers, photovoltaic materials and fluorescent probes.[20]

Dianisole (DAn) is an electron-rich aromatic amine containing two para-methoxy-substituted phenyl rings attached to a central nitrogen atom. The presence of strongly electron-donating methoxy groups enhances the electron density through conjugation making it an efficient electron-donating unit in donor-acceptor systems.[21] In addition, the extended conjugation and strong donating ability facilitate efficient intramolecular charge transfer (ICT) leading to enhanced optical absorption, tunable emission behaviour and improved hole-transport properties.[22] The dianisole derivatives have been widely employed in organic light-emitting diodes (OLEDs), fluorescent probes, photovoltaic devices and other optoelectronic applications.[23]

The electronic nature of the imidazole unit can be effectively modulated depending on the substituent attached at the C2 position. Electron-donating substituents at the C2 position tend to induce electron-deficient character in the imidazole ring, whereas electron-withdrawing substituents can enhance its electron-rich behaviour.[24] This makes imidazole an attractive platform for constructing donor–acceptor (D–A) molecular systems with tunable photophysical properties.[25] Various donor groups such as carbazole, triphenylamine, fluorene, phenothiazine, and anisole derivatives, as well as acceptor units including cyano, benzothiadiazole, pyridine, and triazine moieties, have been incorporated with imidazole frameworks to develop efficient D–A architectures.[26] Such structural modifications promote intramolecular charge transfer (ICT), leading to tunable absorption and emission behaviour, improved charge transport, and enhanced optoelectronic performance for applications in OLEDs, sensing, and organic electronic devices.[27]

1.2. Aim and Strategy of our work

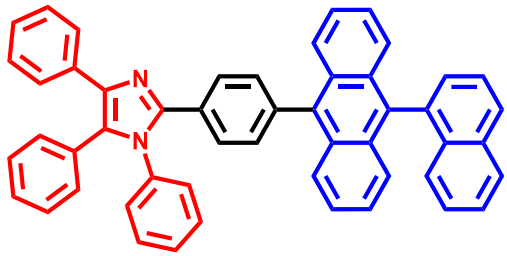
Herein, two 4,5-diphenylimidazole based donor–acceptor systems, **Imd-DAn** and **Imd-Flu**, have been designed and synthesized using dianisole (DAn) and fluorene (Flu) donor units, respectively (Figure 2). In these molecular systems, the DAn and Flu moieties function as electron-donating groups, while the 4,5-diphenylimidazole core acts as the electron-accepting unit. **Imd-DAn** and **Imd-Flu** were synthesized in good yields *via* Buchwald–Hartwig and Suzuki cross-coupling reactions of the dibromo-substituted 4,5-diphenylimidazole precursor (Imd-Br_2) with DAn and Flu-Bpin derivatives, respectively. The synthesized compounds **Imd-DAn** and **Imd-Flu** were characterized using high-resolution mass spectrometry (HRMS), ^{1}H NMR, and ^{13}C NMR spectroscopy.



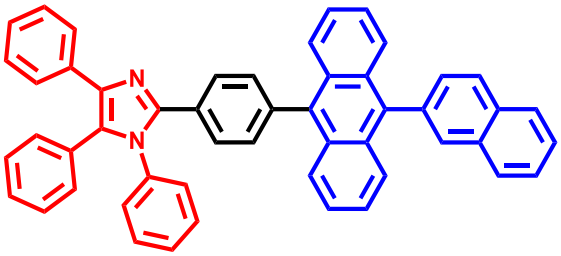
Imd-DAn **Imd-Flu**

Figure 2. The molecular structure **Imd-DAn** and **Imd-Flu**.

In 2012, Wang *et al*. **Imd-1-NaCBI** and **Imd-2-NaCBI** were synthesized *via* Pd-catalysed Suzuki cross-coupling of 2-(4-bromophenyl)-1-phenyl-1H-phenanthro[9,10-d]imidazole with the corresponding naphthyl boronic acid derivatives (Figure 3). **Imd-1-NaCBI** shows absorption and emission maxima at 358 and 431 nm, respectively, while **Imd-2-NaCBI** exhibits slightly red-shifted absorption and emission at 359 and 437 nm. The red shift in **Imd-2-NaCBI** is attributed to improved π-conjugation and enhanced excited-state charge delocalization arising from the different naphthyl substitution pattern. **Imd-1-NaCBI** and **Imd-2-NaCBI** contain similar frontier molecular orbital (FMO) energy levels, with HOMO/LUMO values of -5.25/-2.35 eV for **Imd-1-NaCBI** and −5.24/−2.29 eV for **Imd-2-NaCBI**. These results indicate that slight structural variation in the naphthyl unit influences the photophysical properties of phenanthroimidazole-based systems.[28]



Imd-1-NaCBI

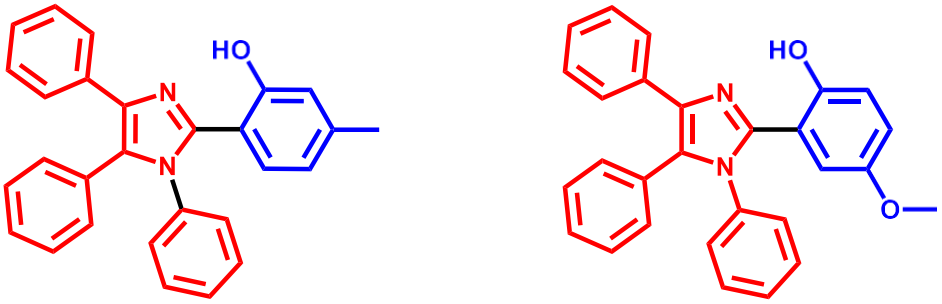


Imd-2-NaCBI

Figure 3. Structures of triphenylimidazole-based OLED emitters **Imd-1-NaCBI** and **Imd-2-NaCBI** with enhanced electroluminescent performance.

In 2013, Park *et al*. **Imd-HPI** and **Imd-m-MHPI** were synthesised *via* Debus–Radziszewski imidazole synthesis by reacting 2-hydroxy-benzaldehyde, 2-hydroxy-4-methoxybenzaldehyde with aniline, benzil, and ammonium acetate in acetic acid under stirring conditions (Figure 4). The introduction of the methoxy substituent in **Imd-m-MHPI** significantly influences the electronic and photophysical properties of the molecule. **Imd-HPI** displays absorption and emission maxima at 319 and 462 nm, respectively, whereas **Imd-m-MHPI** exhibits absorption at 317 nm and a blue-shifted emission at 447 nm. The hypsochromic shift observed for **Imd-m-MHPI** can be attributed to reduced intermolecular interactions and

altered electronic distribution caused by methoxy substitution, which slightly decreases the effective conjugation length. **Imd-HPI** exhibits HOMO/LUMO energy levels of -0.21/-0.97 eV, while **Imd-m-MHPI** shows slightly elevated energy levels of -5.00/-0.87 eV due to the electron-donating nature of the methoxy group. These results demonstrate that electron-donating substituents can effectively tune the electronic structure and emission behaviour of imidazole-based materials.[29]



Imd-HPI **Imd-m-MHPI**

Figure 4. Structures of ESIPT-based imidazole dyes **Imd-HPI** and **Imd-m-MHPI** for full-colour emission applications.

Chapter 3 Experimental Section

3.1. General methods

All reagents and solvents were used as received unless otherwise noted. Moisture-sensitive reactions were performed under an argon atmosphere employing standard Schlenk techniques. Nuclear magnetic resonance (NMR) spectra, including ^{1}H NMR (500 MHz) and ^{13}C NMR (126 MHz) were recorded in $CDCl_3$. Chemical shifts for ^{1}H NMR are reported in ppm relative to the residual solvent peak (δ = 7.26 ppm), with signal multiplicities denoted as singlet (s), doublet (d), or multiplet (m), and coupling constants (J) given in Hz. The chemical shifts for ^{13}C-NMR are given in ppm relative to solvent residual peak ($CDCl_3$, 77.0 ppm). High-resolution mass spectrometry (HRMS) measurements were carried out using ESI-TOF instrumentation operating in APCI mode. UV-visible absorption spectra of the imidazole-based compounds were recorded in dichloromethane (DCM) at a concentration of 1×10^{-5} M using a UV-vis spectrophotometer. In addition, fluorescence emission spectra were measured in DCM using a fluorescence spectrophotometer.

3.2. General procedure for the preparation of the precursors

3.2.1. Synthetic pathway for Compound DAn (3)

A mixture of 1-bromo-4-methoxybenzene (**1**) (0.050 g, 0.144 mol) and 4-methoxyaniline (**2**) (0.036 g, 0.1734 mmol) were dissolved in toluene. Then, it is purged in an inert gas atmosphere for about 15 min, and 0.250g of sodium *tert*-butoxide (t-BuONa) is added. $Pd(OAc)_2$ is added as a catalyst and heated at 110 ℃ for about 48 h. After confirming the completion of the reaction by TLC, the reaction mixture was poured into water and the solvent was removed on a rotavapor. The obtained residue was subjected to column chromatography using DCM: hexane resulting in compound **3** as a white solid with 82% yield. ^{1}H NMR (500 MHz, $CDCl_3$): δ = 6.95 – 6.93 (dd, 4 H), 6.83 – 6.81 (dd, 4 H), 3.78 (s, 6 H). ^{13}C NMR (126 MHz, $CDCl_3$): δ =154.3, 138.0, 119.6, 114.7, 55.7. HRMS (ESI-TOF) Calculated for $C_{65}H_{60}N_2$ m/z $[M]^+$: 230.1176, found: 230.1176.

3.2.2. Synthetic pathway for Compound Imd-Br_2 (7)

Benzil (**4**) (0.3 g, 0.001427 mol), 4-bromoaniline (**5**) (1.23 g, 0.007135 mol) and 4-bromobenzaldehyde (**6**) (0.497 g, 0.001427 mol) were added to a solution of NH_4OAc (0.44 g,

0.005708 mol) in AcOH (15 mL), heated at 118 ℃ for about 24 h. After confirming the completion of the reaction by TLC, the reaction mixture was poured into water, and the solvent was removed on a rotavapor. The obtained residue was subjected to column chromatography using DCM: hexane, resulting in compound **7** as a white solid with 80% yield. ^{1}H NMR (500 MHz, $CDCl_3$): δ = 7.56 (d, J = 7.3 Hz, 2 H), 7.40 (dd, J = 5.5, 8.4 Hz, 4 H), 7.32 - 7.25 (m, 5 H), 7.25 - 7.22 (m, 2 H), 7.22 - 7.17 (m, 1 H), 7.11 (d, J = 6.7 Hz, 2 H), 6.89 (d, J = 8.5 Hz, 2 H), ^{13}C NMR (126 MHz, $CDCl_3$): δ = 145.7, 138.7, 135.9, 134.0, 132.5, 131.5, 131.1, 130.9, 130.4, 130.1, 129.8, 129.2, 128.6, 128.3, 128.2, 127.3, 126.9, 122.9, 122.5. HRMS (ESI-TOF) calculated for $C_{65}H_{60}Br_2N_2$ m/z $[M]^+$: 530.9896, found: 530.9965.

3.2.3. Synthetic pathway for Compound Flu-Bpin (9)

2-bromo-9,9-dipropyl,9-H-fluorene (**8**) (0.4 g, 0.001214 mmol), bis-(pinacolato) diboron (0.617g, 0.002429 mol) was dissolved in 1,4-dioxane in a 100 ml round-bottom flask. Then, it is purged in an inert gas atmosphere for about 15 min and 0.714g of KOAc is added. $Pd(dppf)Cl_2$ is added as a catalyst and heated at 90 ℃ for about 24 h. After confirming the completion of the reaction by TLC, the reaction mixture was poured into water and the solvent was removed on a rotavapor. The obtained residue was subjected to column chromatography using DCM: hexane, resulting in compound **9** as a white solid with 80% yield. ^{1}H NMR (500 MHz, $CDCl_3$): δ = 7.80 (d, J = 7.5 Hz, 1 H), 7.75 (s, 1 H), 7.74 - 7.67 (m, 2 H), 7.38 - 7.29 (m, 2 H), 2.08 - 1.85 (m, 4 H), 1.39 (s, 12 H), 0.69 - 0.56 (m, 10 H). ^{13}C NMR (126 MHz, $CDCl_3$): δ = 151.4, 149.8, 144.1, 140.9, 133.7, 128.9, 128.8, 127.5, 126.7, 122.9, 120.1, 119.0, 83.7, 55.3, 42.6, 24.9, 17.1, 14.4. HRMS (ESI-TOF) calculated for $C_{25}H_{33}BO_2$ m/z $[M]^+$: 377.2656, found: 377.2600.

3.3. Synthetic pathway for Final Compounds

3.3.1. Synthetic pathway for Imd-DAn

Compound **DAn (3)** (0.138 g, 0.0006 mol) and compound **Imd-Br_2 (7)** (0.080g, 0.0001509 mol) were dissolved in toluene in a 100 ml round-bottom flask. Then, it is purged in an inert gas atmosphere for about 15 min and 0.174g of t-BuONa is added. $Pd(OAc)_2$ is added as a catalyst and heated at 110 ℃ for about 48 h. After confirming the completion of the reaction by TLC, the reaction mixture was poured into water and the solvent was removed on a rotavapor. The obtained residue was subjected to column chromatography using DCM: hexane, resulting in **Imd-DAn** as a white solid with 75% yield. ^{1}H NMR (500MHz, $CDCl_3$) :

δ = 7.58 (dd, J = 1.1, 8.3 Hz, 2 H), 7.34 - 7.30 (m, 2 H), 7.27 (br. s., 1 H), 7.25 - 7.20 (m, 4 H), 7.18 - 7.13 (m, 3 H), 7.08 - 7.04 (m, 4 H), 7.01 - 6.96 (m, 4 H), 6.85 - 6.79 (m,12 H), 6.75 - 6.72 (m, 2 H), 3.80 (s,6 H), 3.78 (s, 6 H). ^{13}C NMR (126MHz, CDCl3) : δ = d = 156.2, 156.0, 148.5, 148.4, 147.2, 140.6, 140.3, 137.7, 134.8, 131.2, 131.1, 130.6, 129.5, 129.2, 129.0, 128.2, 128.1, 127.7, 127.4, 126.9, 126.8, 126.3, 122.5, 119.6, 119.3, 114.8, 114.7, 55.5. HRMS (ESI-TOF) calculated for $C_{55}H_{46}N_4O_4$ m/z [M]+ 827.3597, found 827.3336.

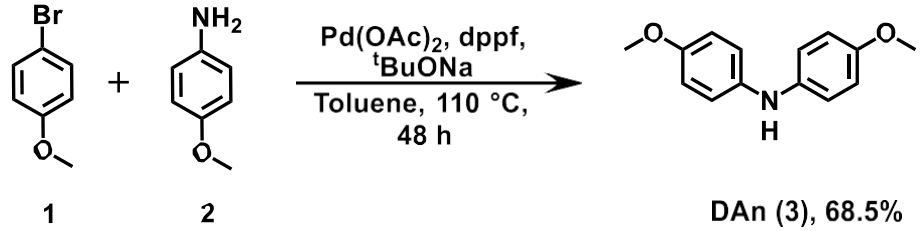
3.3.2. Synthetic pathway for Imd-Flu

Compound **Imd-Br$_2$ (7)** (0.227g, 0.0006035 mol) and compound **Flu-Bpin** (**9)** (0.080g, 0.00015 mol) were dissolved in a 9:3:1 ratio mixture of toluene, ethanol and water in a 100 ml round-bottom flask. Then, it is purged in an inert gas atmosphere for about 15 min, and 0.250g of K2CO3 is added. $Pd(PPh_3)_4$ is added as a catalyst and heated at 90 ℃ for about 24 h. After confirming the completion of the reaction by TLC, the reaction mixture was poured into water and the solvent was removed on a rotavapor. The obtained residue was subjected to column chromatography using DCM: hexane, resulting in compound **Imd-Flu** as a white solid with 61% yield. ^{1}H NMR (500 MHz, $CDCl_3$): δ = 7.79 - 7.67 (m, 4 H), 7.67 - 7.59 (m, 8 H), 7.58 - 7.52 (m, 4 H), 7.40 - 7.31 (m, 8 H), 7.31 - 7.26 (m, 3 H), 7.24 - 7.17 (m, 5 H), 1.97 (br. s.,8 H), 0.66 (20 H). ^{13}C NMR (126 MHz, $CDCl_3$): δ = 151.6, 151.4, 151.0, 146.7, 141.2, 141.2, 141.1, 140.6, 140.4, 139.2, 139.2, 138.6, 138.2, 136.1, 131.2, 131.0, 129.3, 128.7, 128.5, 128.2, 128.0, 127.6, 127.5, 127.3, 127.1, 126.9, 126.8, 126.7, 125.9, 122.9, 122.9, 121.3, 121.2, 121.1, 120.0, 119.9, 119.9, 119.7, 55.4, 55.3, 42.8, 17.2, 14.5. HRMS (ESI-TOF) calculated for $C_{65}H_{60}N_2$ m/z $[M]^+$: 869.4835, found: 869.4837.

Chapter 4 Results and Discussion

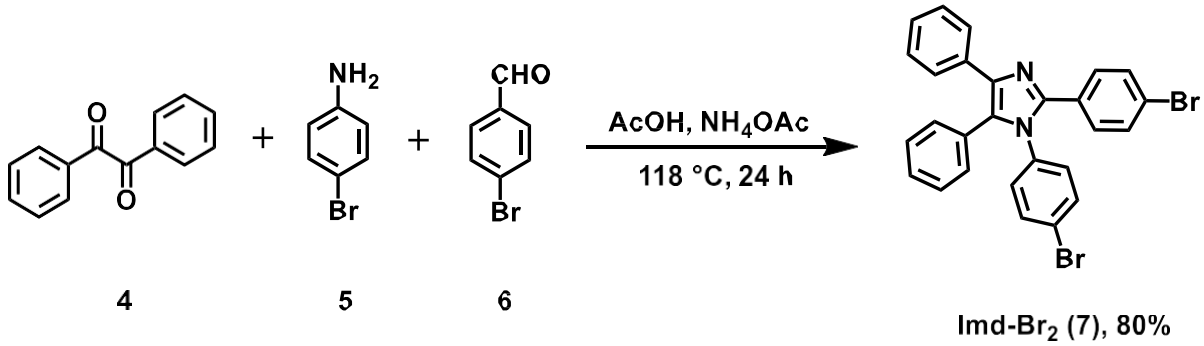
4.1. Synthetic pathway

The DAn (**3**) was synthesized *via* Pd-catalyzed Buchwald-Hartwig cross-coupling reaction of 4-bromoanisole (**1**) with 4-bromoaniline (**2**) using $Pd(OAc)_2$ as the catalyst and ^tBuONa as the base. The reaction was done in toluene at 110 °C for 48 h, affording 68.5% yield (Scheme 1).



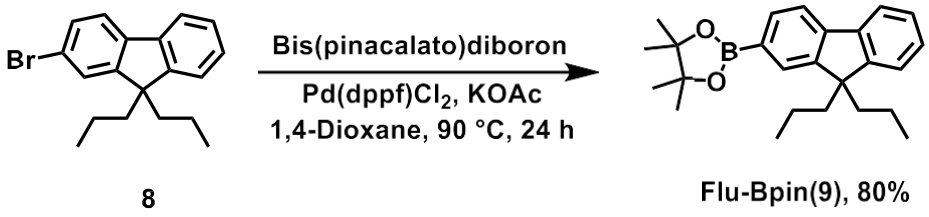
Scheme 1. Synthesis route of **DAn (3)**.

The imidazole derivative Imd-Br_2 (**7**) was synthesized *via* the Debus–Radziszewski imidazole condensation reaction of benzil (**4**), 4-bromoaniline (**5**), 4-bromobenzaldehyde (**6**) and NH_4OAc in acetic acid. The reaction mixture was heated at 118 °C for 24 h, affording 80% yield (Scheme 2).



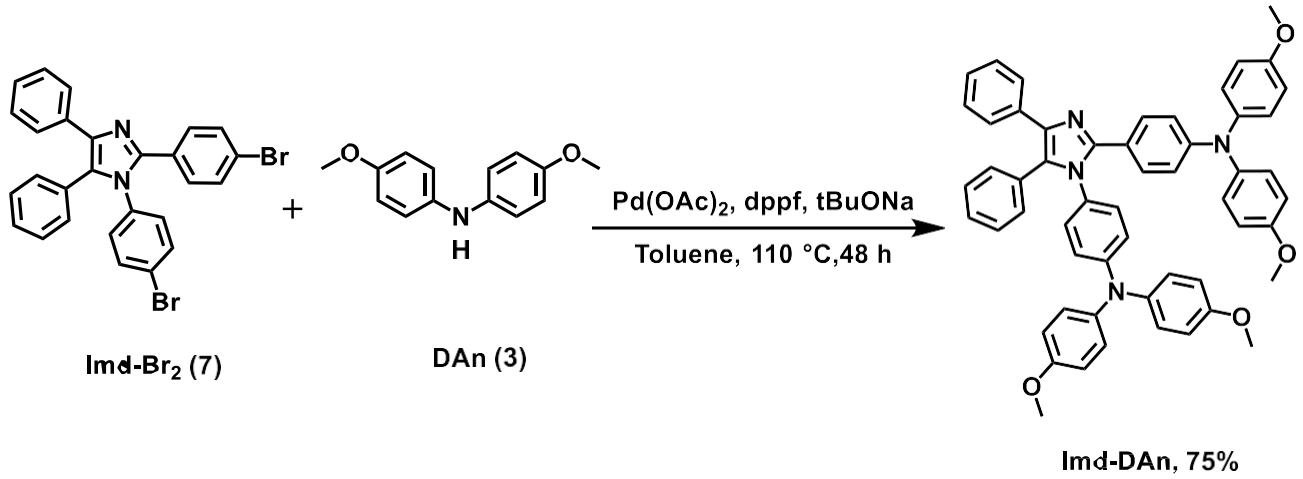
Scheme 2. Synthesis route of **Imd-Br_2 (7)**.

Flu-Bpin (**9**) was synthesized *via* Pd-catalysed Suzuki-Miyaura reaction of 2-bromo-9,9-dipropyl-9H-fluorene (**8**) with Bis(pinacolato)diboron in the presence of $Pd(dppf)Cl_2$ as the catalyst and KOAc as the base. The reaction was heated at 90 °C in 1,4-dioxane solvent for 24 h, affording 80% yield (Scheme 3).



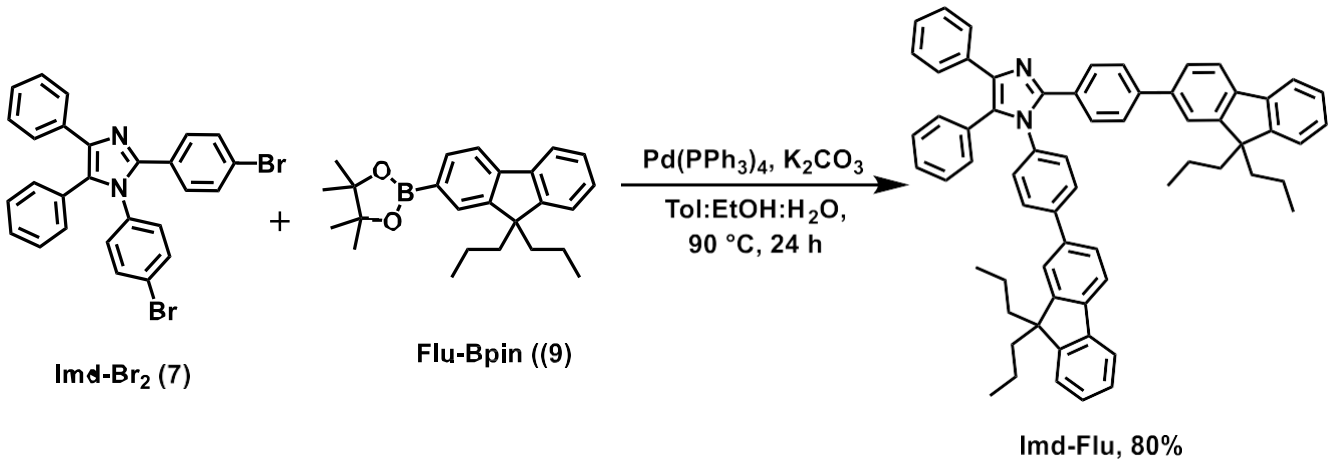
Scheme 3. Synthesis route of **Flu-Bpin** (**9**).

Imd-DAn was synthesised by Buchwald-Hartwig cross-coupling reaction between compound **3** and compound **7** using $Pd(OAc)_2$ as the catalyst and sodium tert-butoxide (t-BuONa) in toluene. The reaction was heated for 110°C for 48 h, affording **Imd-DAn** in 75% yield (Scheme 4).



Scheme 4. Synthesis route of **Imd-DAn**.

Imd-Flu was synthesized *via* Pd-catalyzed Suzuki cross-coupling reaction of Imd-Br_2 (**7**) with Flu-Bpin (**9**) in the presence of [$Pd(PPh_3)_4$] and K_2CO_3 using Tol: EtOH: H_2O as solvent. The reaction was heated at 90 °C for 24 h, affording **Imd-Flu** in 65% yield.



Scheme 4. Synthesis route of **Imd-Flu**

4.2. Photophysical properties

The photophysical properties of dianisole (DAn) and fluorene (Flu) substituted imidazole based donor-acceptor molecules, **Imd-DAn** and **Imd-Flu** were investigated using UV-vis absorption spectroscopy. The absorption spectra of **Imd-DAn** and **Imd-Flu** were recorded in DCM at room temperature using 10^{-5} M concentration and the corresponding spectra are shown in (Figure 5). Both **Imd-DAn** and **Imd-Flu** exhibit absorption bands in the range of 250–350 nm attributed to π–π* electronic transitions. **Imd-DAn** showed an intense absorption maximum at around 340 nm, whereas **Imd-Flu** exhibited an absorption maximum at 320 nm. The absorption spectrum of **Imd-DAn** showed a red shift absorption compared to **Imd-Flu**, which can be attributed to the enhanced π-conjugation and stronger electron-donating nature of the dianisole unit. The emission spectra of **Imd-DAn** and **Imd-Flu** were recorded in DCM solution at room temperature (Figure 6). **Imd-DAn** exhibits two distinct emission maxima centered at 419 nm and 481 nm. In contrast, **Imd-Flu** displays a relatively blue-shifted emission, consisting of shorter-wavelength band at 360 nm along with a broad emission band at 440 nm. The red-shifted and broadened long-wavelength emission of **Imd-DAn** is attributed to the stronger electron-donating ability and enhanced π-conjugation of the dianisole (DAn) unit.

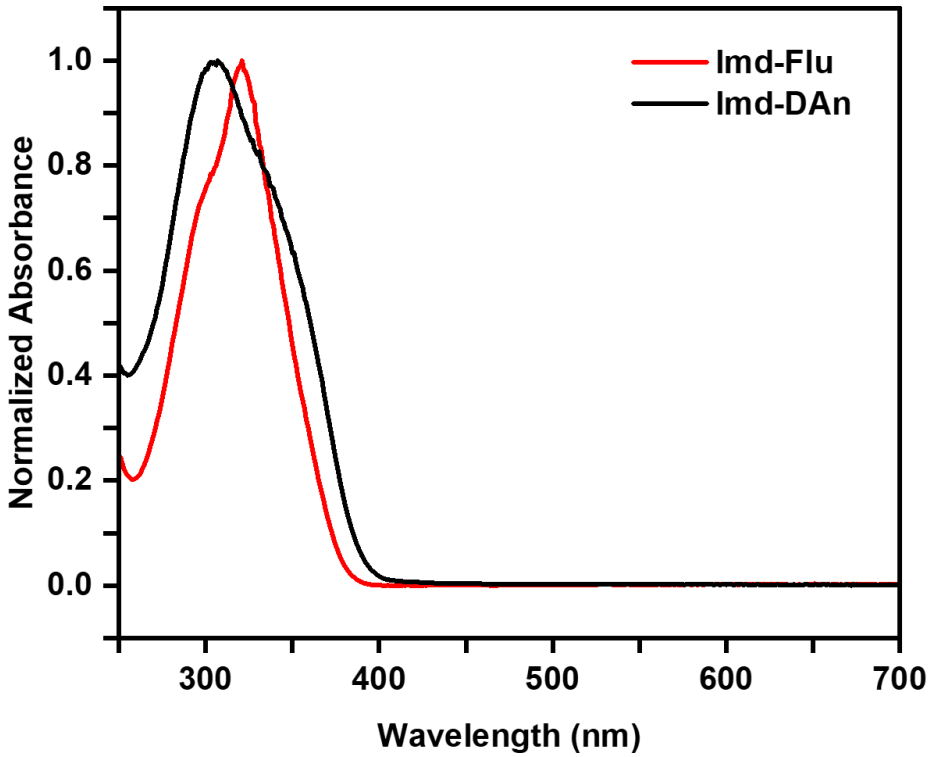


Figure 5. Normalized UV-visible spectra of **Imd-DAn** and **Imd-Flu** and in DCM.

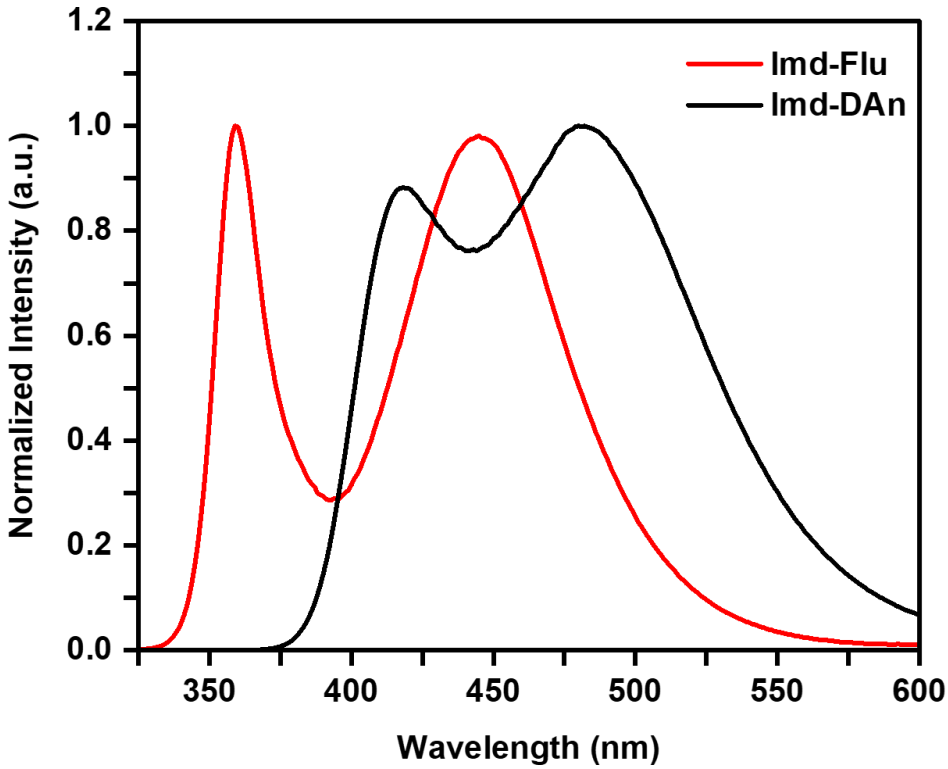


Figure 6. Normalized emission spectra of **Imd-DAn** and **Imd-Flu** in DCM.

4.3. Theoretical calculations

Density functional theory (DFT) calculations were performed to investigate the electronic structure of the imidazole-substituted compounds **Imd-DAn** and **Imd-Flu** using the Gaussian 09W software package. The calculations were carried out employing the B3LYP/6-31G(d,p) basis set. All geometry optimisations and theoretical calculations were conducted in the gas phase. The HOMO of **Imd-DAn** and **Imd-Flu** is mainly localized on the 4,5-diphenylimidazole core and the attached donor units connected at the C2 position of the imidazole ring, while LUMO is delocalized over the entire molecular structure (Figure 7). The calculated energy level diagrams of **Imd-DAn** and **Imd-Flu** are shown in (Figure 8). The HOMO energy levels of **Imd-DAn** and **Imd-Flu** were found to be -5.34 and -4.97 eV , respectively, while the corresponding LUMO energy levels were -1.42 and -0.95 eV. The calculated band gaps for **Imd-DAn** and **Imd-Flu** were found to be 3.22 and 3.92 eV, respectively.

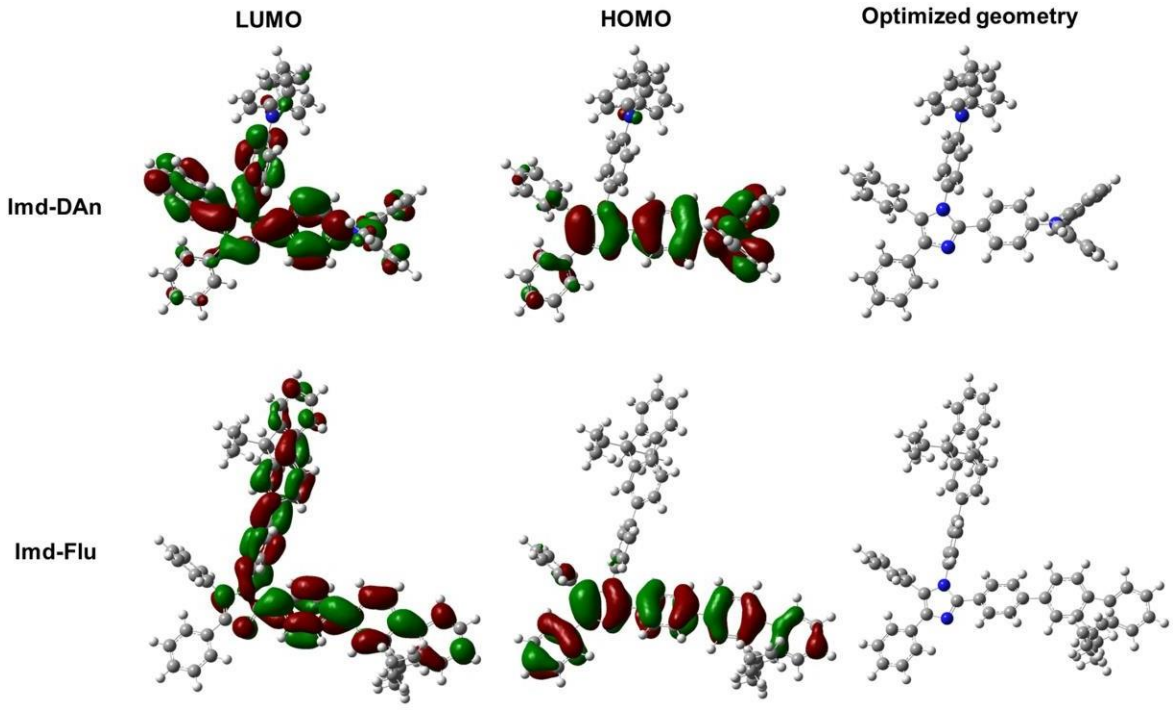


Figure 7. The frontier molecular orbitals (FMO) of the **Imd-DAn** and **Imd-Flu**.

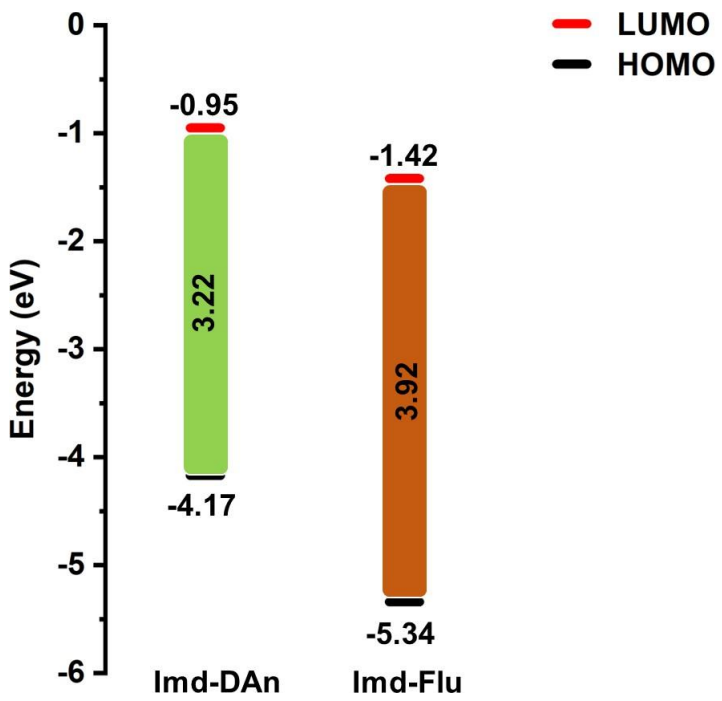


Figure 8. Energy Level Diagram of **Imd-DAn** and **Imd-Flu**.

Chapter 5 Conclusion and Future Scope

5.1. Conclusion

The 4,5-diphenylimidazole fuctionalized donor-acceptor molecules, **Imd-DAn** and **Imd-Flu** were synthesised *via* Buchwald-Hartwig cross coupling amd Suzuki cross-coupling reactions. **Imd-DAn** displayed red shift absorption and emission compared to **Imd-Flu**. DFT calculations demonstrated that the HOMO is mainly localised on the 4,5-diphenylimidazole core and the donor moieties (Flu and DAn) attached at the C2 position of the imidazole unit, while the LUMO is delocalized over the entire molecular framework.

5.2. Future Scope

Further studies of **Imd-DAn** and **Imd-Flu** involving electrochemical analysis, time-resolved fluorescence studies and device fabrication are necessary to establish detailed structure-property relationships and evaluate their applicability in OLEDs, sensing devices and security-related applications such as anti-counterfeiting and information encryption. The present study provides useful insights for the design and development of imidazole-based organic materials with tunable optical and electronic properties for future optoelectronic applications.

APPENDIX-A

Characterization of Compound DAn (3)

1.1 ^{1}H NMR spectrum of Compound DAn (3)

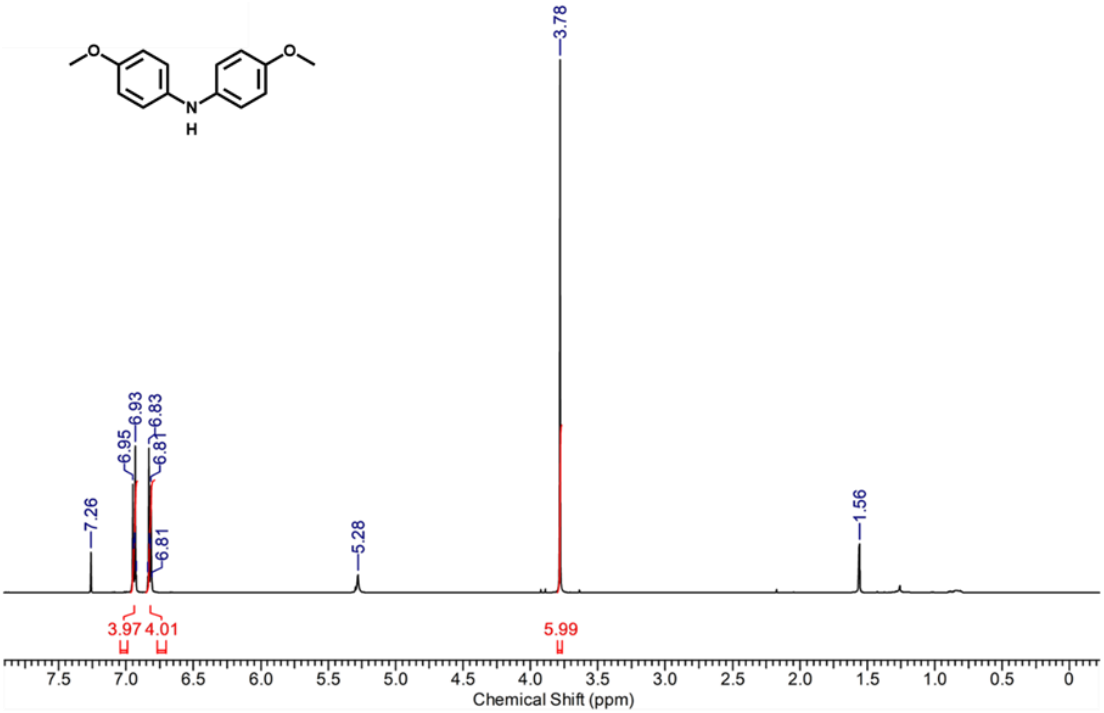


Figure 9. ^{1}H NMR spectrum of Compound **DAn (3)**.

1.2 ^{13}C NMR spectrum of Compound DAn (3)

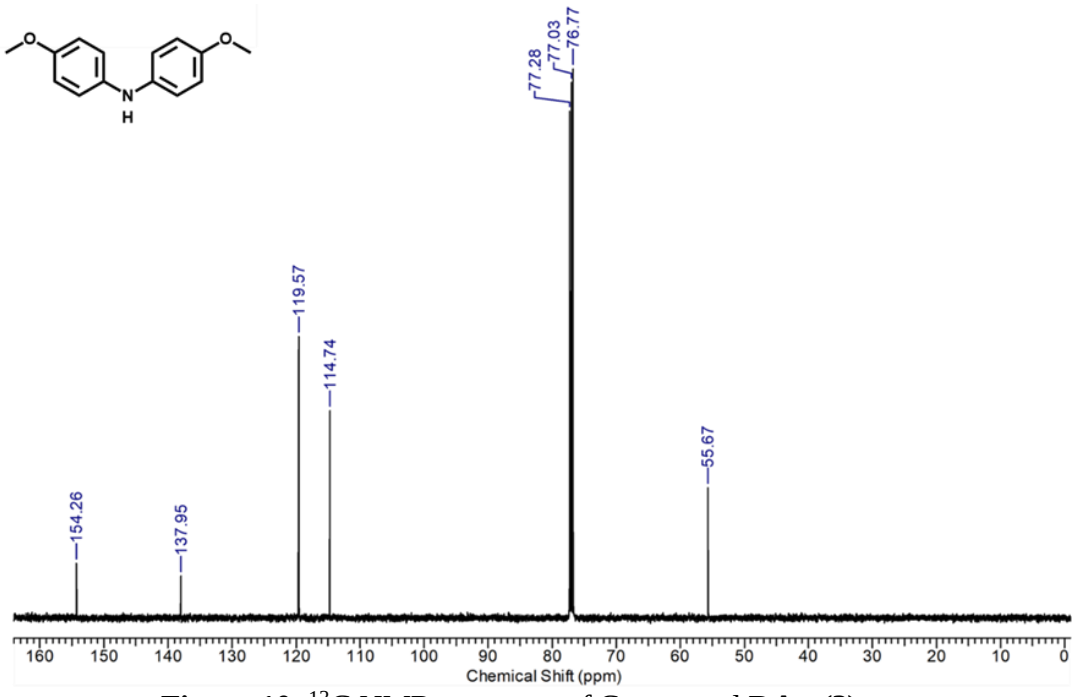


Figure 10. ^{13}C NMR spectrum of Compound **DAn (3)**.

1.3 HRMS of Compound DAn (3)

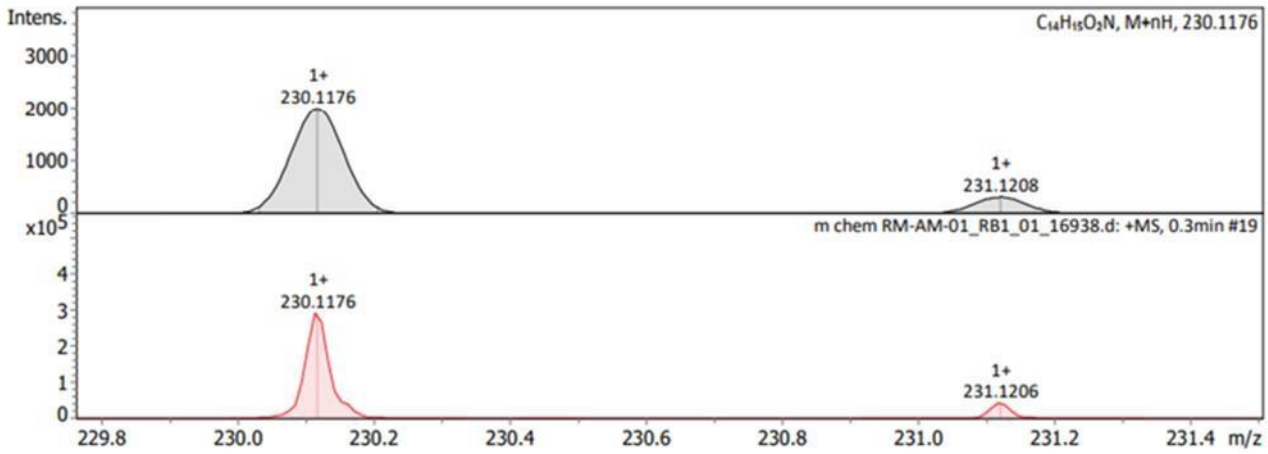


Figure 11. HRMS of Compound **DAn (3)**.

Characterization of Compound Imd-Br_2 (7)

2.1 ^{1}H NMR spectrum of Compound Imd-Br_2 (7)

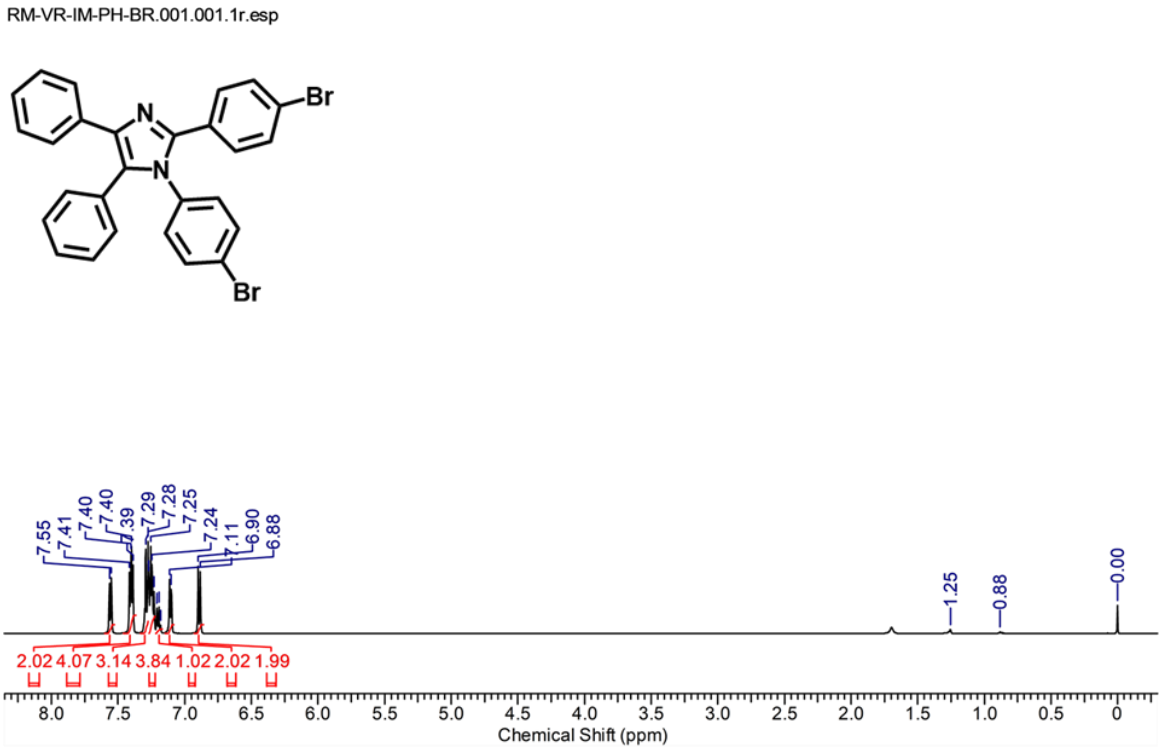


Figure 12. ^{1}H NMR spectrum of Compound **Imd-Br_2 (7)**.

2.2 ^{13}C NMR spectrum of Imd-Br$_2$ (7)

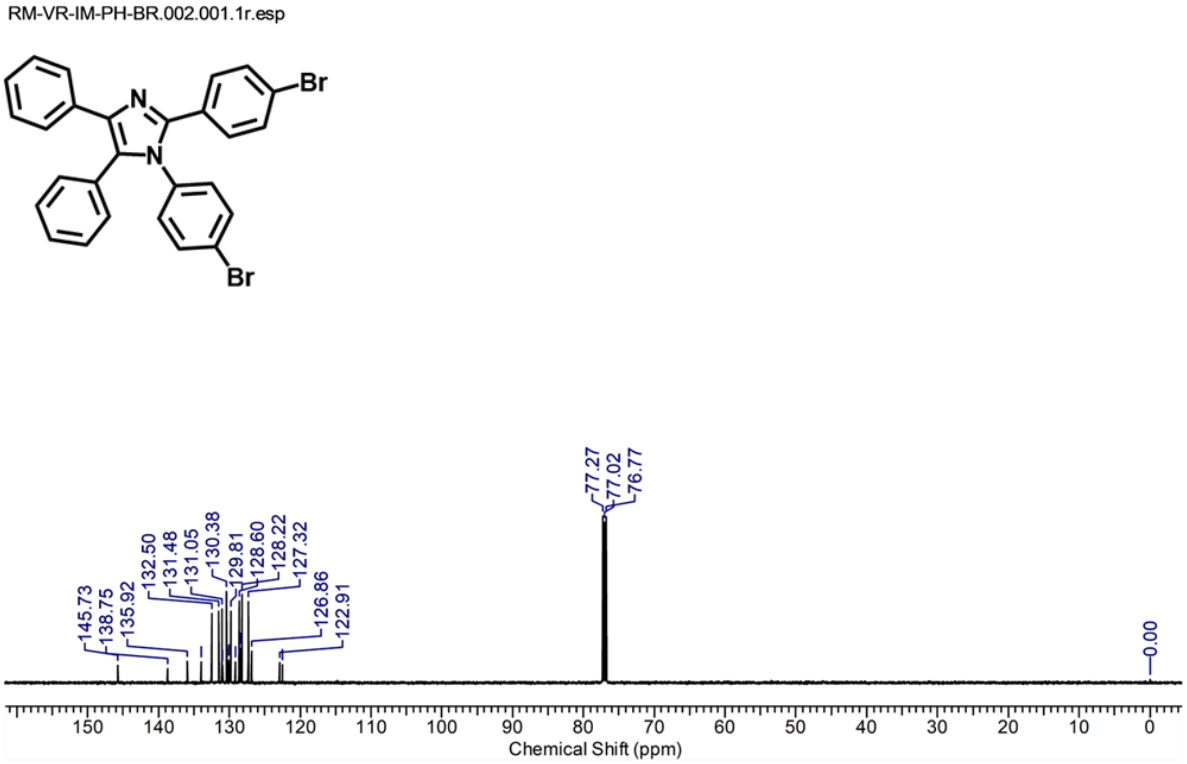


Figure 13. ^{13}C NMR spectrum of Compound **Imd-Br$_2$ (7)**.

2.3 HRMS of Compound Imd-Br$_2$ (7)

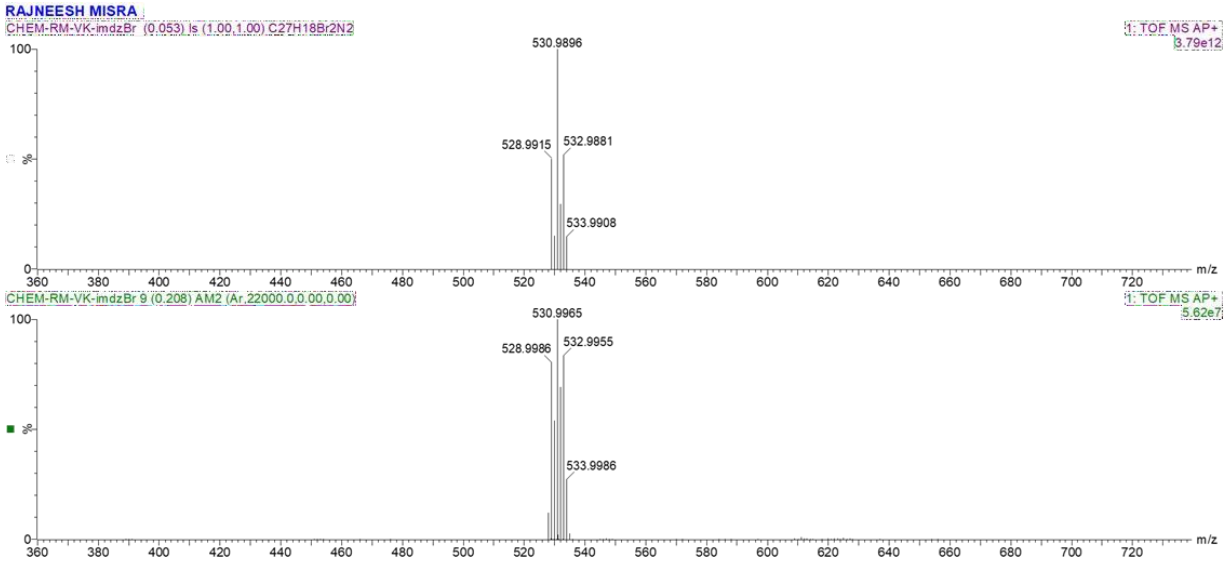


Figure 14. HRMS of Compound **Imd-Br$_2$ (7)**.

Characterization of Compound Flu-Bpin (9)

3.1 ^{1}H NMR spectrum of Compound Flu-Bpin (9)

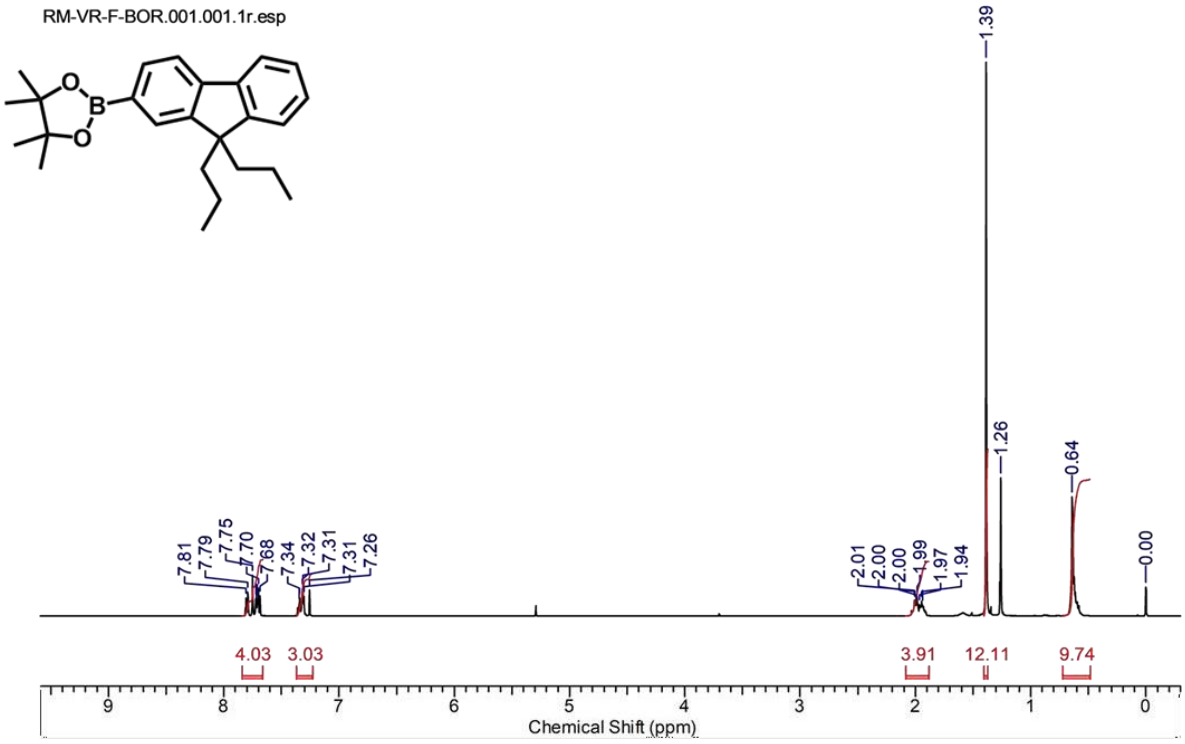


Figure 15. ^{1}H NMR spectrum of Compound **Flu-Bpin (9)**.

3.2 ^{13}C NMR spectrum of Compound Flu-Bpin (9)

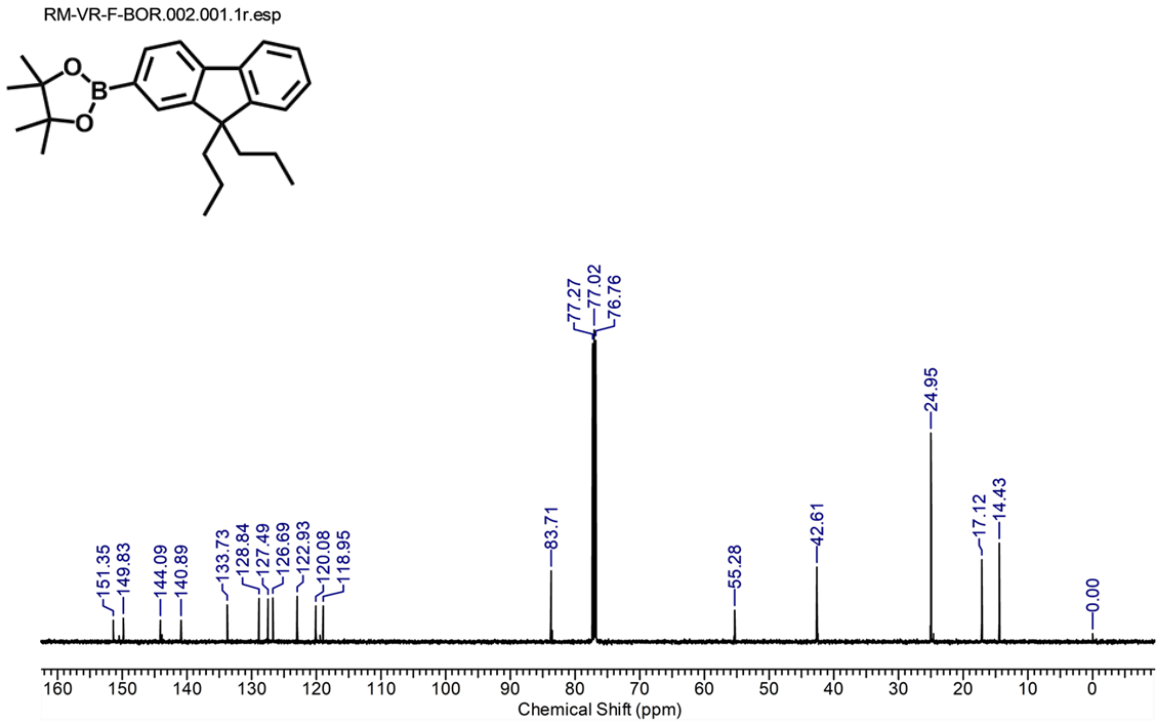


Figure 16. ^{13}C NMR spectrum of Compound **Flu-Bpin (9)**.

3.3 HRMS of Compound Flu-Bpin (9)

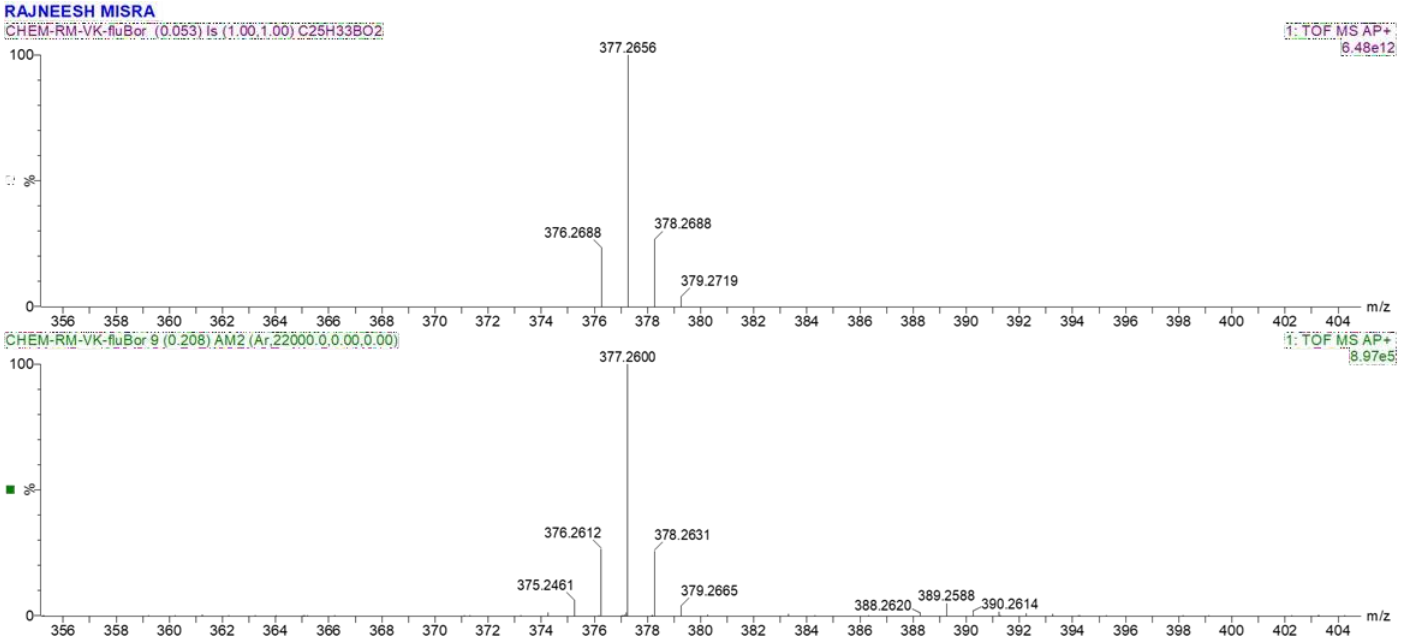


Figure 17. HRMS of Compound **Flu-Bpin (9)**.

Characterization of Compound Imd-DAn

4.1 ^{1}H NMR spectrum of Compound Imd-DAn

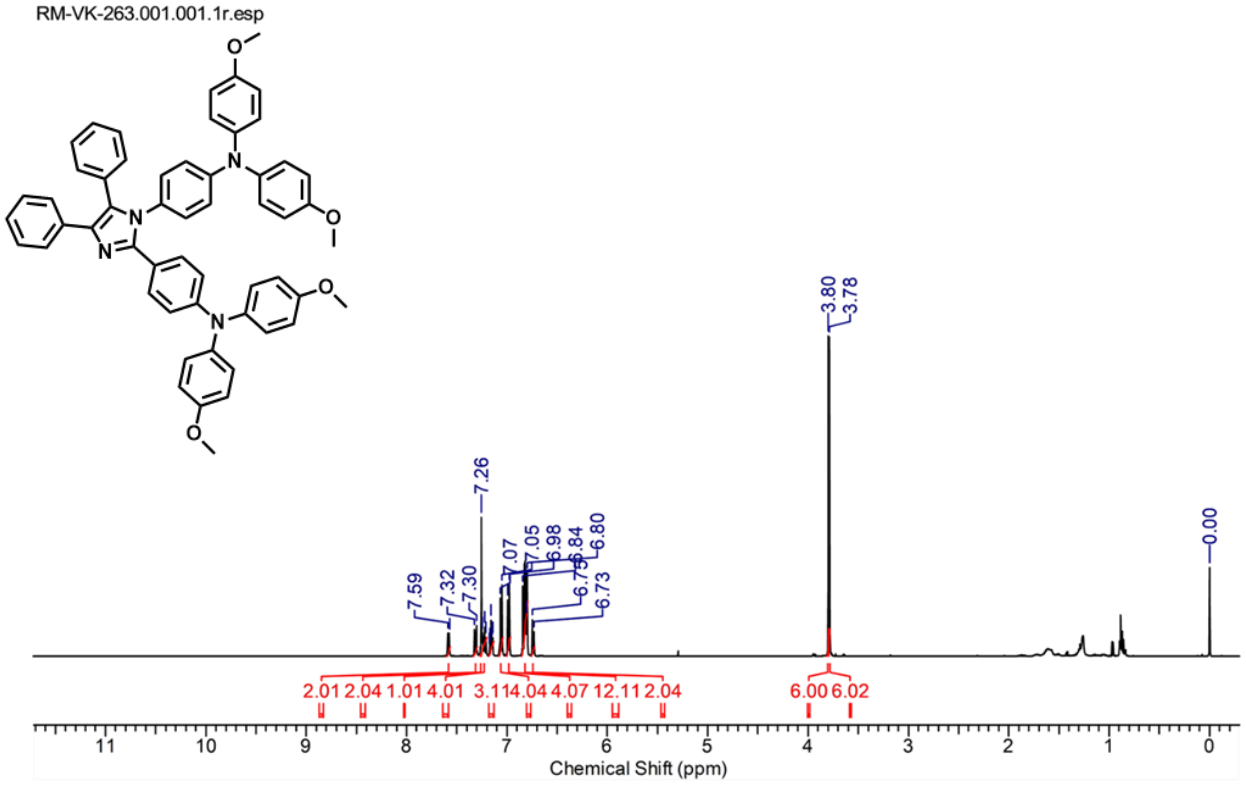


Figure 18. ^{1}H NMR spectrum of Compound **Imd-DAn**.

4.2 ^{13}C NMR spectrum of Compound Imd-DAn

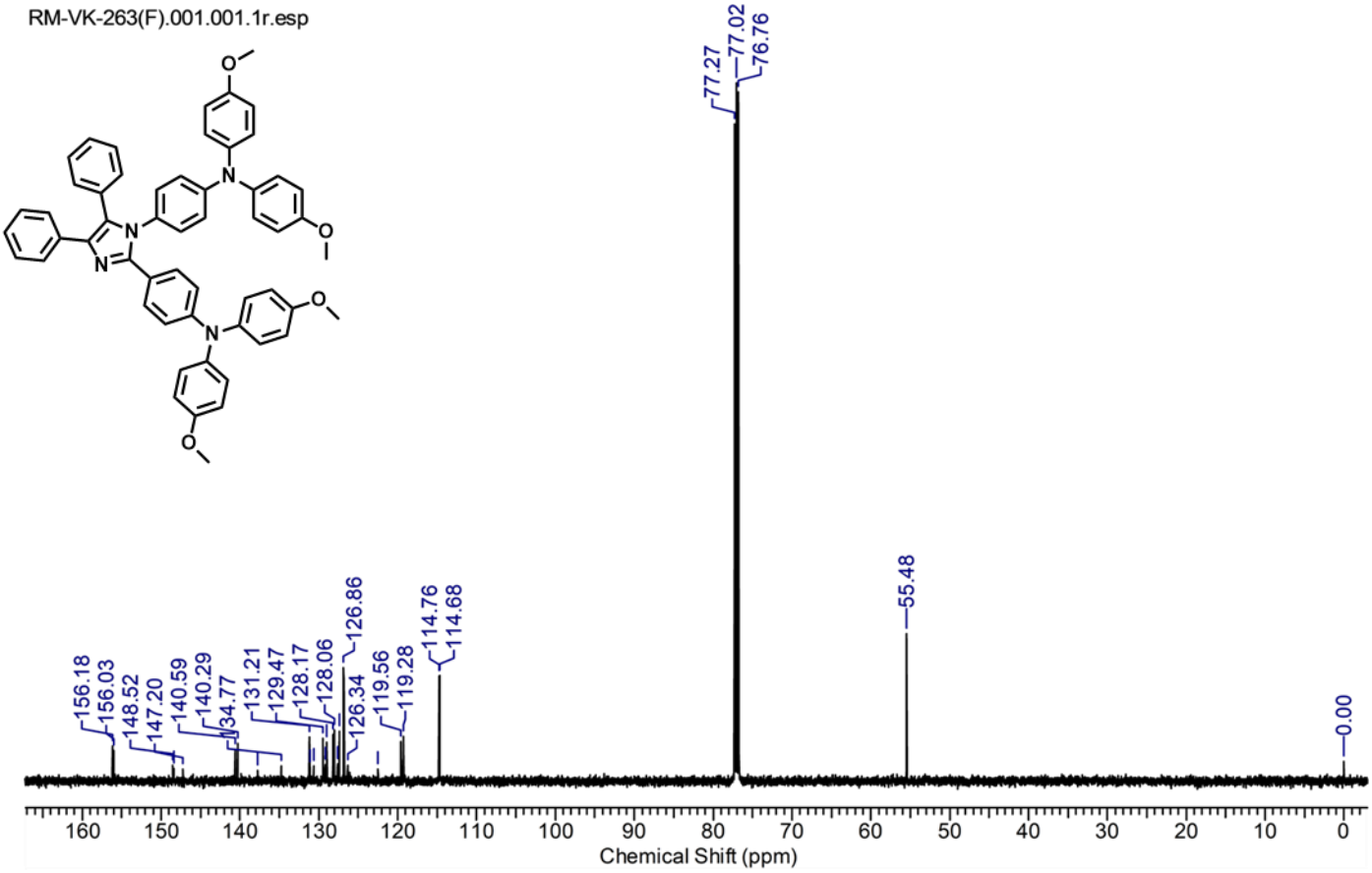


Figure 19. ^{13}C NMR spectrum of Compound **Imd-DAn**.

4.3 HRMS of Compound Imd-DAn

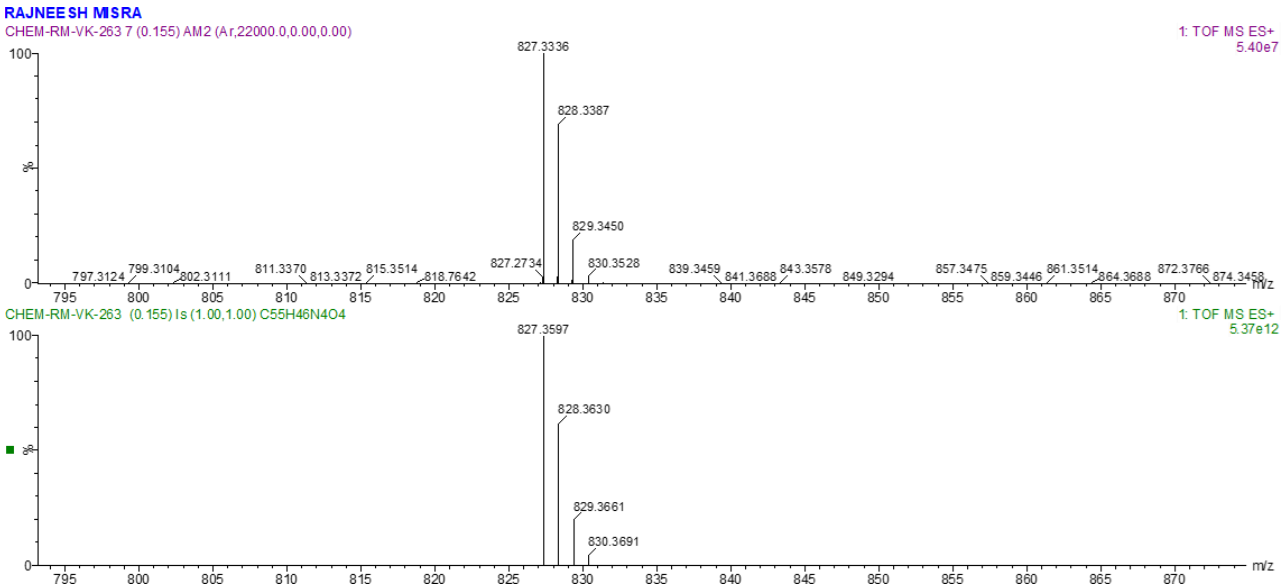


Figure 20. HRMS of Compound **Imd-DAn**.

Characterization of Compound Imd-Flu

5.1 ^{1}H NMR spectrum of Compound Imd-Flu

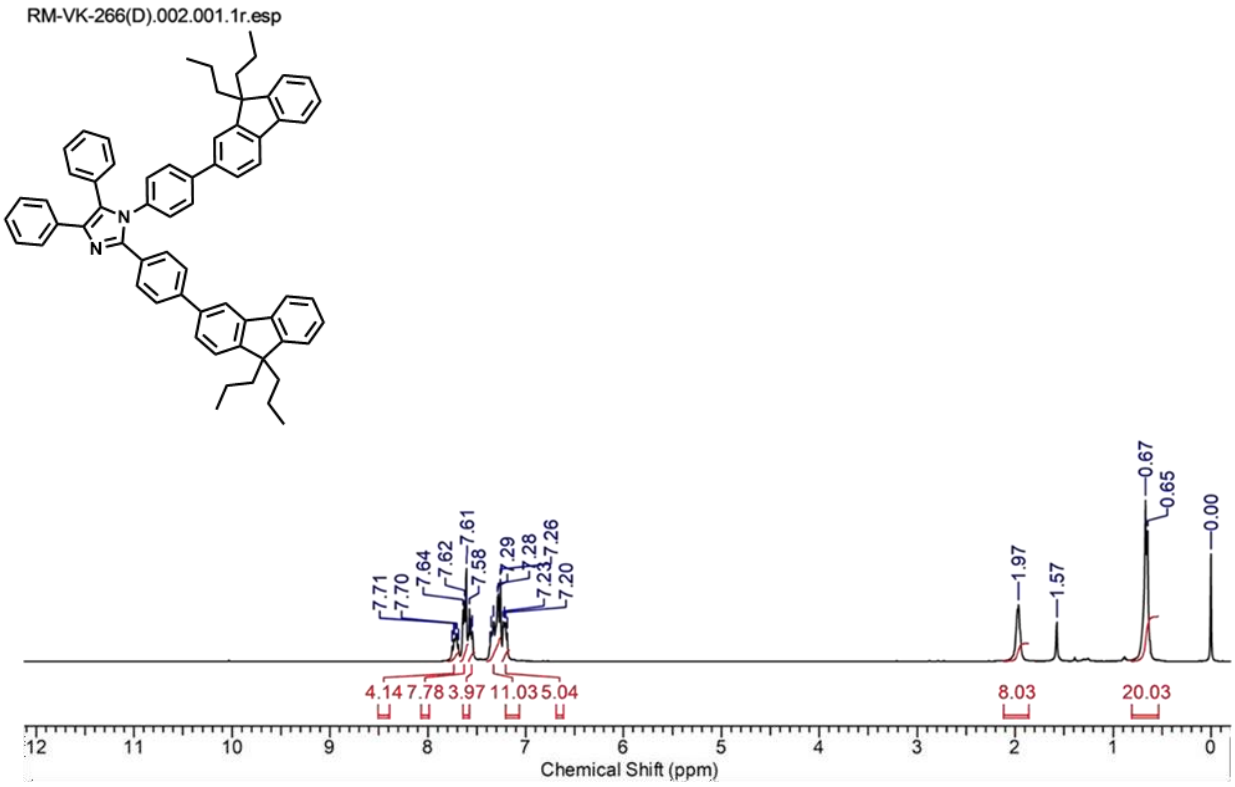


Figure 21. ^{1}H NMR spectrum of Compound **Imd-Flu**.

5.2 ^{13}C NMR spectrum of Compound Imd-Flu

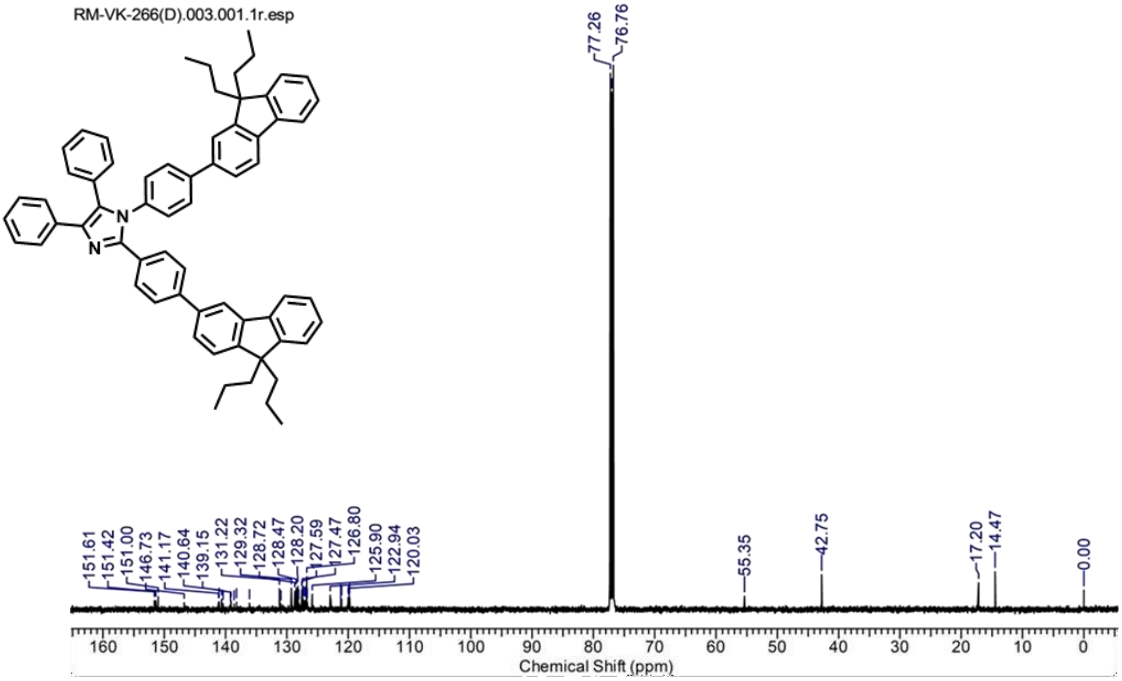


Figure 22. ^{13}C NMR spectrum of Compound **Imd-Flu**.

5.3 HRMS of Compound Imd-Flu

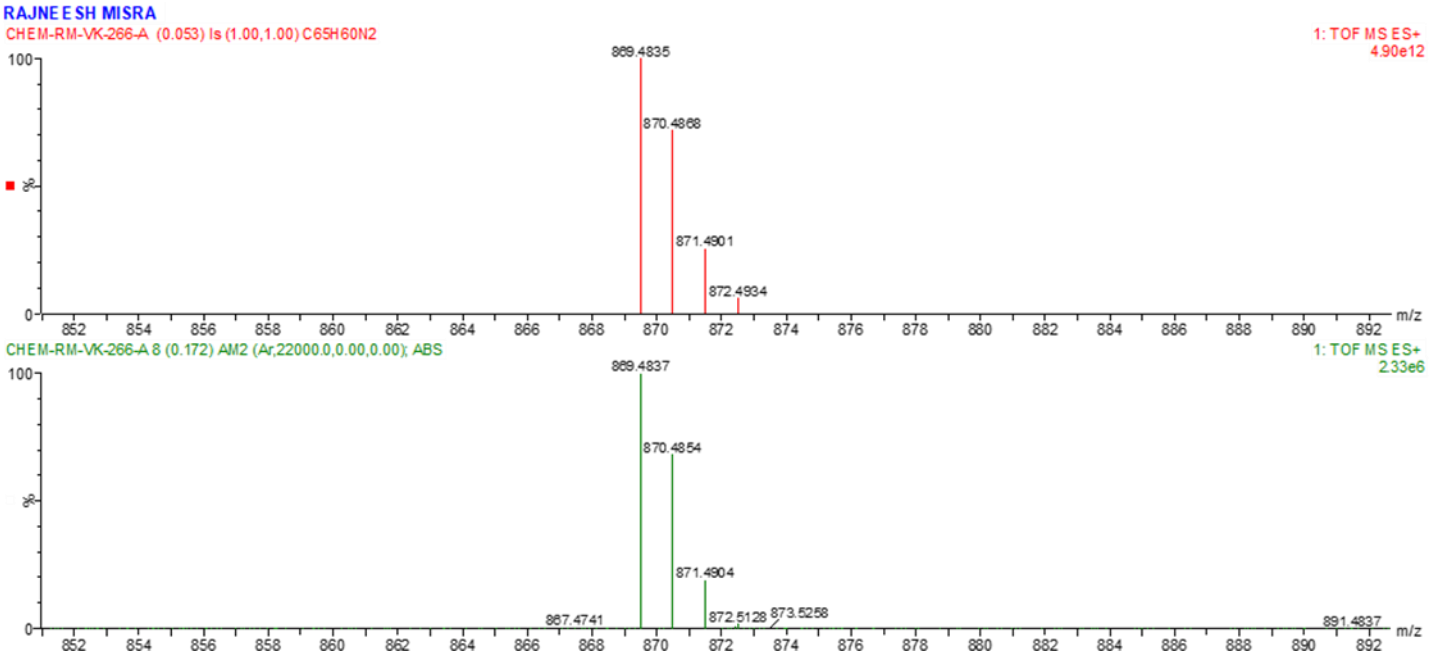


Figure 23. HRMS of Compound **Imd-Flu**.

REFERENCES

[1] Z.-H. Guo, Z.-X. Jin, J.-Y. Wang and J. Pei, A Donor–Acceptor–Donor Conjugated Molecule: Twist Intramolecular Charge Transfer and Piezochromic Luminescent Properties, *Chem. Commun.*, **2014**, *50(46*), 6088–6090.

[2] R. Misra, T. Jadhav, B. Dhokale and S. M. Mobin, Reversible Mechanochromism and Enhanced AIE in Tetraphenylethene Substituted Phenanthroimidazoles, *Chem. Commun*., **2014**, *50(65)*,9076–9078.

[3] F. Khan, A. Ekbote, S. M. Mobin and R. Misra, Mechanochromism and Aggregation-Induced Emission in Phenanthroimidazole Derivatives: Role of Positional Change of Different Donors in a Multichromophoric Assembly, *J. Org. Chem.*, **2021**, *86(2)*, 1779–1792.

[4] T. Jadhav, J. M. Choi, J. Shinde, J. Y. Lee and R. Misra, Mechanochromism and Electroluminescence in Positional Isomers of Tetraphenylethylene Substituted Phenanthroimidazoles, *J. Mater. Chem. C***, 2017**, *5(24)*, 6014–6020.

[5] T. Jadhav, B. Dhokale, Y. Patil, S. M. Mobin and R. Misra, Multi-Stimuli Responsive Donor–Acceptor Tetraphenylethylene Substituted Benzothiadiazoles, *J. Phys. Chem. C*, **2016**, *120(42)*, 24030–24040.

[6] M. Poddar, G. Sivakumar and R. Misra, Donor–Acceptor Substituted 1,8-Naphthalimides: Design, Synthesis, and Structure–Property Relationship, *J. Mater. Chem. C*, **2019**, *7(47)*, 14798–14815.

[7] J. Yang, J. Huang, Q. Li and Z. Li, Blue AIEgens: Approaches to Control the Intramolecular Conjugation and the Optimised Performance of OLED Devices, *J. Mater. Chem. C*, **2016**, *4(14)*, 2663–2684.

[8] Z. Zhang, Q. Wang, X. Zhang, D. Mei and J. Mei, Modulating the Luminescence, Photosensitizing Properties, and Mitochondria-Targeting Ability of D–π–A-Structured Dihydrodibenzo[a,c]Phenazines, *Molecules*, **2023**, *28(17)*.

[9] J. Mahar, G. Shabir, P. A. Channar, A. Saeed, K. D. Belfield, M. Irfan and A. Ul-Hamid, Donor-Pi-Acceptor Fluorene Conjugates, Based on Chalcone and Pyrimidine Derivatives: An Insight into Structure-Property Relationship, Photophysical and Electrochemical Properties, *J. Fluoresc*., **2020**, *30(2)*, 419–426.

[10] S. Zhuang, R. Shangguan, J. Jin, G. Tu, L. Wang, J. Chen, D. Ma, and X. Zhu, *Org. Electr*. **2012**, *13*, 3050–3059.

[11] E.Kwon, S. Park, and S.Y. Park, *J. Am. Chem. Soc.*, **2013**, *135*, 11239-11246.

[12] W.-C. Chen, Y. Yuan, Y. Xiong, A. L. Rogach, Q.-X. Tong and C.-S. Lee, Aromatically C6- and C9-Substituted Phenanthro[9,10-d]Imidazole Blue Fluorophores: Structure–Property Relationship and Electroluminescent Application, *ACS Appl. Mater. Interfaces*, **2017**, *9(31)*, 26268–26278.

[13] S. Park, J. E. Kwon and S. Y. Park, Strategic Emission Color Tuning of Highly Fluorescent Imidazole-Based Excited-State Intramolecular Proton Transfer Molecules, Phys. *Chem. Chem. Phys.*, **2012**, *14(25)*, 8878–8884.

[14] S. Ye, Z. Shaoqing, P. Biao, G. Runda and L. Wang, Imidazole Derivatives for Efficient Organic Light-Emitting Diodes, *J. Inf. Disp*., **2020**, *21(3)*, 173–196.

[15] P. Molina, A. Tárraga and F. Otón, Imidazole Derivatives: A Comprehensive Survey of Their Recognition Properties, *Org. Biomol. Chem*., **2012**, *10(9)*, 1711–1724.

[16] T.-Y. Wu, M.-H. Tsao, F.-L. Chen, S.-G. Su, C.-W. Chang, H.-P. Wang, Y.-C. Lin, W.-C. Ou-Yang and I.-W. Sun, Synthesis and Characterization of Organic Dyes Containing Various Donors and Acceptors, *Int. J. Mol. Sci*., **2010**, 329–353.

[17] N. T. S. Phan, M. Van Der Sluys and C. W. Jones, On the Nature of the Active Species in Palladium Catalysed Mizoroki–Heck and Suzuki–Miyaura Couplings – Homogeneous or Heterogeneous Catalysis, A Critical Review, *Adv. Synth. Catal*., **2006**, *348(6)*, 609–679.

[18] Wang, D. Xin, L. Zhenni, L. Guangyan, H. Shili and S. Hou, Imidazole Compounds: Synthesis, Characterisation, and Application in Optical Analysis, *Crit. Rev. Anal. Chem*., **2024**, *54(5)*, 897–922.

[19] Y.-D. Lin, W.-W. Tsai and C.-W. Lu, Exploring the Electroluminescent Applications of Imidazole Derivatives, *Chem. – A Eur. J.*, **2023**, *29(23)*, e202203040.

[20] A. Kundu, S. Karthikeyan, D. Moon and S. P. Anthony, Synthesis of Strongly Fluorescent Imidazole Derivatives: Structure Property Studies, Halochromism and Fluorescent Photoswitching, *J. Fluoresc.*, **2019**, *29(6)*, 1359–1369.

[21] S. S. Reddy, W. Cho, V. G. Sree and S.-H. Jin, Multi-Functional Highly Efficient Bipolar 9,9-Dimethyl-9,10-Dihydroacridine/Imidazole-Based Materials for Solution-Processed Organic Light-Emitting Diode Applications, *Dyes Pigm*., **2016**, *134*, 315–324.

[22] S. Petdee, C. Chaiwai, W. Benchaphanthawee, P. Nalaoh, N. Kungwan, S. Namuangruk, T. Sudyoadsuk and V. Promarak, Imidazole-Based Solid-State Fluorophores with Combined ESIPT and AIE Features as Self-Absorption-Free Non-Doped Emitters for Electroluminescent Devices, *Dyes Pigm.*, **2021**, *193*, 109488.

[23] B. P. Debata, M. D. Thiyagarajan, P. R., J. D. Girase, S. K. Iyer, S. Patel and S. Vaidyanathan, Benzil-Imidazole Blue Fluorophores and Their Applications in Blue/White Light-Emitting Diodes, Sensing and Anticounterfeiting, *J. Mater. Chem. C*, **2025**, *13(6)*, 2711–2731.

[24] J. D. Girase, S. Singh, B. P. Debata, S. R. Nayak, M. R. Nagar, J.-H. Jou, S. Patel and S. Vaidyanathan, Structural Engineering of Deep-Blue Emitters (Imidazoles Integrated with Triphenylamine) Leads to EQE > 6% and High Colour Purity (CIEy ∼ 0.09) for Solution-Processed OLEDs, *J. Phys. Chem. C*, **2023**, *127(33)*, 16623–16635.

[25] J. Devesing Girase, S. Rani Nayak, J. Tagare, Shahnawaz, M. Ram Nagar, J.-H. Jou and S. Vaidyanathan, Solution-Processed Deep-Blue (Y∼0.06) Fluorophores Based on Triphenylamine-Imidazole (Donor-Acceptor) for OLEDs: Computational and Experimental Exploration, *J. Inf. Disp*., **2022**, *23(1)*, 53–67.

[26] K. Kumar, D. Sharma, D. Thakur, A. Karmakar, H.-W. Yang, J. Jayakumar, S. Banik, J.-H. Jou and S. Ghosh, Sterically Crowded Donor-Rich Imidazole Systems as Hole Transport Materials for Solution-Processed OLEDs, *Langmuir*, **2024**, *40(10)*, 5137–5150.

[27] W. Li, D. Liu, F. Shen, D. Ma, Z. Wang, T. Feng, Y. Xu, B. Yang and Y. Ma, A Twisting Donor-Acceptor Molecule with an Intercrossed Excited State for Highly Efficient, Deep-Blue Electroluminescence, *Adv. Funct. Mater*., **2012**, *22(13)*, 2797–2803.

[28] J. Jayabharathi, P. Nethaji, V. Thanikachalam and R. Ramya, Derivatives of Cyanonaphthyl-Substituted Phenanthroimidazole as Blue Emitters for Nondoped Organic Light-Emitting Diodes, *ACS Omega*, **2019**, *4(3)*, 4553–4570.

[29] G. Chen, Z. Qiu, J.-H. Tan, W.-C. Chen, P. Zhou, L. Xing, S. Ji, Y. Qin, Z. Zhao and Y. Huo, Deep-Blue Organic Light-Emitting Diodes Based on Push-Pull π-Extended Imidazole-Fluorene Hybrids, *Dyes Pigm*., **2021**, *184*, 108754.

[30] X. Shao, N. Zhou, F. Xun, J. Liu, H. Lin and L. Wang, Triphenylamine-Phenylimidazole-Based Hybridised Local and Charge-Transfer Molecular as Blue-Green/ White Light Emission Emitter for Light-Emitting Diode Application, *J. Lumin*., **2024**, *267*, 120391.

[31] B. Debata, S. Patel and S. Vaidyanathan, Imidazo[1,5-a]Pyridine-Benzilimidazole Conjugated (Donor–π–Acceptor) Greenish-Yellow Fluorophores and Their Applications in White Light-Emitting Diodes, Acidochromism and Anticounterfeiting, *J. Mater. Chem. C*, **2025**, *13*, 10413–10433.

[32] S. R. Nayak, S. Patel and S. Vaidyanathan, Imidazole-Based Fluorescent Probes: Concomitant Effects of N1 Substitution and Lone Pair on Selective Recognition of Picric Acid, New J. Chem., 2023, 47(7), 3524–3534.

[33] S. Manoj Kumar and S. Kulathu Iyer, D–π–A–π–D-Configured Imidazole-Tethered Benzothiadiazole-Based Sensor for the Ratiometric Discrimination of Picric Acid: Applications in Latent Fingerprint Imaging, *J. Org. Chem*., **2024**, *89(8)*, 5392–5400.

[34] Z. Yu, S. Liu, H. Zhang, S. Liu, G. Shi, K.-P. Wang, S. Chen and Z.-Q. Hu, Polyaryl Substituted Imidazobenzothiadiazoles as Multifunctional Organic Fluorescent Materials for Visualisation of Latent Fingerprints and Lysosome Staining, *Dyes Pigm.*, **2023**, *214*, 111213.

[35] S. M. Kumar, S. Munusamy, D. Jothi, S. Enbanathan and S. K. Iyer, Rationally Constructed Imidazole Derivatized Schiff-Base Based Fluorescent Sensor for Reversible Identification of Copper Ions and Its Applications in Fingerprint Imaging, *J. Mol. Liq*., **2023**, *373*, 121235.

[36] Debata, B. P.; Patel, S.; Vaidyanathan, S. Fluorophores with imidazole building blocks and their multifunctional platforms for optoelectronics (LEDs/OLEDs), chemo-sensing, and security applications: recent advances and future perspectives. *J. Mater. Chem. C*, **2026**, *14*, 5141–5176.